Journal of Earth Science, *Vol. 33*, *No. 2*, *p. 236−256*, *April 2022* *ISSN 1674-487X*
Printed in China
https://doi.org/10.1007/s12583-021-1532-x

Classification of Sandstone-Related Uranium Deposits

Michel Cuney*[1], Julien Mercadier[1], Christophe Bonnetti[2]
1. *Université de Lorraine*, *GéoRessources*, *CNRS*, *CREGU*, *Nancy F*54500, *France*
2. *State Key Laboratory of Nuclear Resources and Environment*, *East China University of Technology*, *Nanchang* 330013, *China*
Michel Cuney: https://orcid.org/0000-0002-8201-4398

ABSTRACT: Sandstone type deposits are the most common type of uranium deposits in the world. A large variety of sub-types have been defined, based either on the morphology of the deposits (e.g., tabular, roll front, etc), or on the sedimentological setting (e.g., paleovalley, paleochannel, unconformity), or on tectonic or lithologic controls (e.g., tectonolithologic, mafic dykes/sills), or still on a variety of others characteristics (phreatic oxidation type, interlayer permeable type, multi-element stratabound infiltrational, solution front limb deposit, humate type, etc.), reflecting the diversity of the characteristics of these deposits, but making it difficult to have a clear overview of these deposits. Moreover, uranium deposits occurring in the same sedimentological setting (e.g., paleochannel), presenting similar morphologies (e.g., tabular), may result from different genetic mechanisms and thus can be misleading for exploration strategies. The aim of the present paper is to propose a new view on sandstone-related uranium deposits combining both genetic and descriptive criteria. The dual view is indeed of primordial importance because all the critical characteristics of each deposit type, not limited to the morphology/geometry of the ore bodies and their relationships with depositional environments of the sandstone, have to be taken into account to propose a comprehensive classification of uranium deposits. In this respect, several key ore-forming processes, like the physical-chemical characteristics of the mineralizing fluid, have to be used to integrate genetic aspects in the classification. Although a succession of concentration steps, potentially temporally-disconnected, are involved in the genesis of some uranium mineralization, the classification here proposed will focus on the main mechanisms responsible for the formation and/or the location of ore deposits. The objective of this paper is also to propose a robust and widely usable terminology to define and categorize sandstone uranium deposits, considering the diversity of their origin and morphologies, and will be primarily based on the temperature of the mineralizing fluid considered as having played the critical role in the transportation of the uranium, starting from synsedimentary uranium deposits to those related to higher temperature fluids.
KEY WORDS: sandstone, uranium, genetic classification, redox control, depositional environment, fluids, ore deposit geology.

0 INTRODUCTION

Sandstone uranium deposits, also referenced as sandstone related deposits, represent by far the most common type of uranium deposits (662 deposits out of the 1 807 deposits listed in the UDEPO database; IAEA, 2016) and are known on every continent. The most recent classification of sandstone-hosted uranium deposits is the one proposed by the IAEA (2018a, b), integrating previous classification attempts such as those of de Voto (1978), Nash et al. (1981), Dahlkamp (2009, 1993), and IAEA (2009). Sandstone-hosted uranium deposits occur in a large diversity of sedimentary settings, from medium- to coarse-grained sandstone deposited in a continental fluvial, lacustrine to lagunar conditions, or in channel, lagoonal, and beach-bar settings on the marginal plains of marine sedimentary environments. More rarely, uranium deposits may also occur in sandstone of eaolian origin. Distribution of uranium and associated elements (e.g., V, Cu, Zn) are considered to be controlled by oxidation states of the sandstones layers as well as oxidizing water flow, which is chiefly controlled by sandstone porosity, connectivity, and permeability. The fluids in these deposits are diverse, with variable oxidation states (oxidizing or reducing) and with different origins: meteoric waters, diagenetic brines, fluids migrated from hydrocarbon reservoirs or emanating from a crystalline basement. Circulation of oxidizing uraniferous and/or reducing fluids may be driven by gravity (topography or salinity-related density controls), compaction, convection, hydrodynamic regime (Chi and Xue, 2014), or tectonic processes such as basin inversion (Cheng et al., 2020 for roll front deposits; Cui et al. (2012) for basement/basin redox controlled deposits) or seismic pumping (Sibson et al., 1975) proposed for basin/basement redox controlled deposits. The uranium deposition in sandstone uranium deposits are mainly driven by circulation of fluids and distribution of redox barrier

*Corresponding author: michel.cuney@univ-lorraine.fr

Manuscript received May 6, 2021.
Manuscript accepted August 17, 2021.

but, where lacustrine rocks and fine-grained organic-rich sediments dominate, the uranium deposits may be in part or entirely syngenetic related to synsedimentary to early diagenetic concentrations.

Uranium and associated redox sensitive elements are precipitated either directly by intrinsic reducing agents occurring within the sandstone, such as carbonaceous material, sulphides, Ti-Fe-oxides, and ferro-magnesium minerals in the sandstone or as basic volcanic layers or dykes, or by extrinsic reduced compounds (fluids, bitumen, gas) infiltrated through faults, or directly (i.e., biomineralisation) and indirectly through bacterial sulphate reduction (e.g., Kyser and Cuney, 2015).

Sandstone uranium deposits are considered by some authors as restricted to post-Silurian sediments, because of their genetic relation with the presence of detrital vascular land plants involved directly or indirectly in the deposition of uranium (Finch and Davis, 1985). However, the existence of sandstone uranium deposits in which the reductants are minerals trapped in rocks or fluids migrated from oil/gas reservoir opens up the time frame during which these deposits could have formed. In this respect, sandstone uranium deposits have been formed for almost 2 Ga, with the oldest occurrence known in the Franceville Basin in Gabon. Although they do not represent the oldest uranium concentrations on Earth, sandstone uranium deposit are among the types of U deposits with a presence among the longest known. Pre-2.2 Ga uranium mineralization are known in Archean and Lower Paleoproterozoic coarse siliciclastic rocks (conglomerates), but they will not be included in the present paper because they do not involve redox processes as all other sandstone related uranium deposits.

Sandstone uranium deposits have been classically divided into five major sub-types (IAEA, 2018a): (i) basal channel deposits hosted in wide paleochannels filled with poorly sorted alluvial-fluvial unconsolidated sediments and generally occurring in narrow valleys. Ore bodies usually form elongated ribbons or lenses, and more rarely present a roll shape. The uranium is essentially associated with detrital plants. The typical deposits of this type are those of the Vitim district in Russia (Kochkin et al., 2017). They are also referred to as phreatic oxidation type by the Soviet and Chinese geologists; (ii) roll-front deposits with a typical crescent-shape ore bodies in cross section, but occasionally with a more complex morphology. They are developed at the interface (front) between originally reduced and secondarily oxidized poorly lithified arkosic sandstone between aquicludes. They typically present a color zoning. In plane section the ore bodies are snake-shaped and elongated nearly parallel to the strike of the sedimentary strata. Roll front deposits are classified as "interlayer permeable type" associated to an "interlayer oxidation zone" by Soviet and Chinese geologists (Jin et al., 2020; Pechenkin, 2014), "multi-element stratabound infiltrational" (Schmariovich et al., 1988), or as "solution front limb deposits" by Klingmuller, (1989). For most of them the reductant is intrinsic and represented by detrital carbonaceous debris (Bonnetti et al., 2020), but for some of them the reductant is extrinsic and derived from underlying hydrocarbon reservoirs (e. g., South Texas; Hall et al., 2017). The sandstones are deposited in intracratonic or intermontane basins, in the vicinity of U-rich granites and tuffs containing anomalous uranium concentrations (e. g., deposits from the Wyoming or Australia), or in continental to marginal marine setting (e.g., Chu-Sarisu and Syr-Daria basins, Kazakhstan, Mathieu et al., 2015), or still in marginal marine environment (e. g., South Texas, Hall et al., 2017); (iii) tabular deposits forming irregularly shaped sheet-like ore bodies, with an elongation parallel to the depositional trend. They occur in more or less consolidated fluvial to fluvial-lacustrine sandstone or siltites, rich in organic matter, and intercalated with shale. A more or less important pyroclastic contribution may be present. Uranium is commonly associated with elevated contents of V, Mo, Cu, Zn and/or Zr. Typical deposits are those of the Arlit district in Niger and those of the Colorado Plateau (USA, Sanford, 1992). In the Grants Region (USA), an extrinsic origin of the humate/bitumen has been proposed but is controversial (Turner-Peterson and Fishman, 1986); (iv) tectonic/lithologic deposits with ore bodies hosted in sediments rich in organic matter are controlled both by sedimentary and tectonic structures. The reductants can be intrinsic (detrital organic matter) or extrinsic (migrated hydrocarbons). Lodève in France (Mathis et al., 1990) and Oklo in Gabon (Gauthier-Lafaye et al., 1989) are considered as the reference examples for tectonic/lithologic uranium deposits; and (v) mafic dykes/sills in Proterozoic sandstones in which the location and shape of the ore bodies are controlled by the presence of mafic dykes and/or sills injected in the sandstones (e. g., Westmoreland District, Australia, Polito et al., 2005).

The generic term "sandstone deposit" covers consequently a great variety of deposits occurring in a diversity of geological environments and generated following a variety of physical and chemical conditions, and thus cannot be used appropriately without further qualification to define a deposit type. This classification of sandstone uranium deposits (IAEA, 2018a) is dominantly based on the morphology/geometry of the uranium ore bodies and to some extend to their relationships with the depositional environments of the sandstone. However, sandstone uranium deposits presenting similar morphologies may result from a variety of physical-chemical-biological processes associated for instance with the circulations of a large variety of fluids with variable Eh, pH, temperature, and salinity. Such classification does not consider the genetic processes at the origin of the deposit and is therefore badly adapted to define uranium exploration strategies. A striking evidence is the deposits hosted by the FA sandstone of the Franceville Basin, in Gabon, which are currently classified in the tectonic/lithological category of IAEA (2018a). They were formed in fact in rather equivalent genetic conditions as the so called unconformity-related deposits from Canada and Australia, but as the latter are not systematically hosted by sandstone, the two types of deposits are consequently attributed to a different deposit category in most classifications. In addition, sandstone uranium deposits are considered in most classifications as resulting from epigenetic processes, whereas some of them may be essentially of synsedimentary origin. Moreover, synsedimentary deposits generally have a tabular shape, but differing from a genetic aspect from that of the classical tabular deposits as defined above. Another problem caused by previous classifications are the terms basal channel or paleovalley setting used for a urani-

um deposit, which can be also attributed to uranium deposits of the calcrete type. Moreover, the definition of calcrete uranium deposit is based on an implicit genetic concept, i.e., the evapotranspiration process at the origin of the calcrete, but not on the shape of the ore body or the nature of the host rock as used for conventional descriptive deposit-type classification. To finish this list of examples, metamorphosed sandstone deposits are classified in the category of metamorphic deposits, but in fact most of them belong to one or the other type of the sandstone uranium deposit group, but have been later variably modified by metamorphism.

Considering these limitations, the aim of the present paper is to propose a new view on sandstone-related uranium deposits combining both genetic and descriptive criteria. The dual view is indeed of primordial importance because all the critical characteristics of each deposit type, not limited to (but taking them into consideration mainly for the definition of sub-types) the morphology/geometry of the ore bodies and their relationships with depositional environments of the sandstone, have to be taken into account to propose a comprehensive classification of uranium deposits. In this respect, several key ore-forming processes, like the physical-chemical characteristics of the mineralizing fluid, have to be used to integrate genetic aspects in the classification. The classification cannot be based entirely on the depositional environments, which may have a strong control on the localization of certain types of sandstone related deposits, but have no specific role in others. Although a succession of concentration steps, potentially temporally-disconnected, are involved in the genesis of some the uranium mineralization as currently observed, the classification here proposed will focus on the main mechanisms responsible for the formation and/or the location of ore deposit. The objective of this paper is also to propose a robust and widely usable terminology to define and categorize sandstone uranium deposits, considering the diversity of their origin and morphologies. The order of presentation of the six deposit types will be primarily based on the temperature of the mineralizing fluid considered as having played the critical role in the transportation of the uranium, starting from synsedimentary uranium deposits to those related to higher temperature fluids.

1 SYNSEDIMENTARY-EARLY DIAGENETIC SANDSTONE SYSTEMS

Uranium can be incorporated either in mudstone-dominated sediments rich in organic matter during their deposition or early diagenesis, such as peat, coal and black shales, or in phosphorites, but uranium can be also deposited syngenetically in organic matter-bearing sandstone and siltstone (Bonnetti et al., 2015a). The critical question being if such synsedimentary to early diagenetic processes have been sufficient to generate significant economic or sub-economic mineralization or if they lead only to the formation of low grade preconcentrations which need to be reworked by other processes to form economic uranium deposits. For example, a syngenetic uranium precipitation in a reduced sedimentological environment has been proposed for some of the tabular uranium deposits, in particular those from Niger by Cazoulat (1985). However, all recent studies attribute the origin of the economic mineralization to much later diagenetic processes, which will be discussed later, without denying that a part of the uranium may be initally of synsedimentary origin.

The best example to illustrate synsedimentary uranium deposits hosted in sandstone is the relatively large Nehuting deposit (estimated resources of about 10 000 t U at 0.03% to 0.1% U, Dahlkamp, 2009), in the northern part of the Erlian Basin, in northern China (Bonnetti et al., 2015a). It is dominantly hosted in quartz-rich siltstone to silty mudstone of the Late Cretaceous Erlian Formation, which were deposited within fluvial-lacustrine environment. Uranium mineralization is considered as first concentrated in wetland environments, adsorbed on clay mineral surfaces, Fe-Ti oxides and hydroxides and organic matter. UO_2^{2+} is initially adsorbed on organic material and subsequently reduced (Nakashima et al., 1987). Then, UO_2 forms nano- to micro-crystals disseminated in the clayey matrix and organic matter. Synsedimentary/early diagenetic uranium is remobilized during late diagenesis almost *in situ* and redeposited locally as pitchblende and P-rich coffinite or as replacement of pyrite crystals and pyritized organic matter. The presence of framboidal pyrite and the phosphorus-rich nature of the coffinite indicate that uranium deposition results from H_2S production by sulfate-reducing bacteria. Only a minor part of the U mineralization has been remobilized during an epigenetic stage of cementation because of the very poor permeability of the host silty-mudstone. Synsedimentary uranium mineralization is also known in other locations in the Erlian Basin (e. g., Naomugen and Subeng deposits, Dahlkamp, 2009) as well as significant primary uranium preconcentrations (30.4 ppm U in average and up to 70 ppm) within the organic matter-, Fe-sulphide-rich sandstones in the Saihan Formation, which represent a sort of proto-ore for the Bayinwula roll front deposits (Bonnetti et al., 2015b). In addition, similar syngenetic to diagenetic uranium preconcentrations were also characterized in sandstones of the Yaojia Formation, which were considered as a major source of uranium for the epigenetic tabular deposits in the southern Songliao Basin in north China (Bonnetti et al., 2017).

A dominantly syngenetic origin is also proposed for the Mulga rock uranium deposits hosted in the Eocene Ambassador paleochannel along the southwestern margin of the Gunbarrel Basin at the western margin of the Officer Basin, Western Australia (Douglas et al., 2011). Uranium resources are estimated at more than 30 000 t U at grades of 400 ppm to 600 ppm. Uranium associated with a series of elements (Cu, Ni, Co, Se, Pb) have been first concentrated within reduced lacustrine to paludal carbonaceous sands and clays with peat-derived lignite and clay-rich lignite layers. Uranium occurs mainly as diffuse concentrations associated with organic matter or clay minerals, with rare occurrence of coffinite and U-oxide. This last deposit is transitional with the lignite-coal uranium deposit type, but these deposits differ by the association of uranium with massive coal and lignite layers and a subordinate occurrence of sandstone layers.

These syngenetic deposits (Nehuting and Mulga Rocks) are classified as tabular sandstone deposits by Dahlkamp (2009) and in the IAEA UDEPO data base, in the same category as the deposits of Niger or Colorado which have yet a very

different origin and geologic setting. Hence, using only the morphological aspect to classify these deposits is not sufficient because incorrect, and leads to confusion.

2 METEORIC FLUID INFILTRATION SYSTEMS

Five sub-types of uranium deposits derive essentially from the solubilization of uranium by meteoric fluid infiltration ("exogenic infiltration" from the Russian authors) and its deposition at low temperature within highly permeable siliciclastic sediments. The persistence of moderately dipping, continuous strata, associated to basin uplift allowing for slow percolation of groundwater and a permeable environment are essential for the genesis of economic uranium deposits linked to meteoric infiltration systems.

2.1 Evapotranspiration

Deposits formed by meteoric near-surface phreatic waters, occur dominantly in paleovalleys and to a lesser extend in playa lake settings, filled with Tertiary to Quaternary coarse, angular, and poorly sorted organic matter free, cobbles, gravels and sandstone, with little evidence of chemical weathering. Palaeovalleys are incised in basement rocks, and form relatively narrow steep-walled channels. The climatic conditions were hot and varied from arid to semi-arid with sporadic rainfall (Carlisle, 1984). Such rainfall could also be occasionally torrential causing deposition of poorly sorted immature conglomerates, sometime with large boulders as at Langer Heinrich in Namibia. They are most commonly cemented by variable amounts of carbonates, with near-surface deposition of uranyl-vanadates in arid to semi-arid desertic conditions. They are commonly referred to as calcrete uranium deposits in the literature but similar deposits may present a different cement: dolocrete, gypcrete, silcrete and other authigenic material (e. g., Chudasama et al., 2018; Cuney and Kyser, 2015; Carlisle, 1984). Most if not all economic deposits are of the calcrete type. The mineralization occurs generally as tabular ribbon-shaped ore bodies (e. g., 6 km long, 500 m wide and 8 m thick for the Yeleerie deposit in Western Australia, Cameron et al., 1980). The main uranium mineralization occurs where bed rock highs and a constriction of the valley width decreases drainage, causing the migration of the water table closer to the evaporative surface. The migration of the phreatic waters to the atmosphere induces evaporation of these waters and subsequent oversaturation and precipitation of uranyl vanadate minerals in valley calcrete or playa lake siliciclastic sediments. The transfer of the phreatic water to the surface also occur as a transpiration through the pores of the siliciclastic formation in response to the dehydration of the upper part of the sediments by evaporation, evaporation induced by the high surface temperature due to arid climatic conditions. Mixing between uranyle-carbonate bearing waters with waters containing dissolved vanadium species is also a possible additional mechanism (Chudasamaa et al., 2018). The term "evapotranspiration deposits" is considered as it is the most common feature shared by all these deposits and which is not recognized in any other uranium deposit type.

2.2 Sealed Paleovalleys

Sealed paleovalleys deposits correspond to deposits occurring in paleovalleys filled with Tertiary to Quaternary coarse and poorly sorted sandstone, but rich in organic matter unlike the previous type, and generally sealed by basalt layers. They are related to meteoric water infiltration and hosted in sandstone between impermeable layers like roll front deposits, but they do not display the classical horizontal redox zonation of these deposits and display a tabular shape. The so-called basal channel deposits are associated to this category of deposit in the IAEA classification (IAEA, 2018a) but these deposits occur near the base of much larger basins than the preceding ones and are associated to much better sorted sandstone units and are not sealed by volcanic rock. They are hosted in paleochannels and have a tabular shape, descriptive characteristics which can be observed within several other types of uranium deposits, such as the so called tabular deposits of Niger or Colorado, calcrete deposits ("calcrete palaeochannel deposits of Namibia" of Bowell et al., 2009), and syngenetic deposits (e.g., Mulga Rocks, Western Australia). Hence, the so-called basal channel uranium deposits will not be considered in the sealed paleovalley category.

2.3 Valley Confined Amalgamated Sandy Meander Belts (VC-ASMB)

Uranium deposits of this category will regroup mineralization that were named in the previous classification as "basal channel". These deposits occur in large sedimentary basins (e. g., Callabonna sub-basin, South Australia with the Beverley deposit, Western Chinle Basin, USA with the Monument Valley and White Canyon uranium districts), but they are confined into alluvial paleovalley meander belts, where the fluvial channel and related overbank flood are not connected with adjacent interfluves (Hartley et al., 2018). A series of these paleovalleys can be amalgamated as in the case of the Shinarump member of the Chinle Formation in the USA. The ore bodies are tabular to lenticular shaped nearly conformable to the bedding and enlongated parallel to scour trends. The Australian Beverley deposit hosted in Miocene sediments is of Pliocene age (Wulser et al., 2011). It has never been buried to more than a few hundreds of meters and the occurrence of framboidal pyrite attests a bacterial activity connected to the genesis of the deposits, implying low temperature conditions (<50 °C). It clearly results from meteoric water infiltration at relatively shallow depth. The depth at which the deposits hosted in the Shinarump sandstone have been formed is more difficult to precise because the age of uranium deposition is not very well constrained. Some authors have proposed a synsedimentary origin (Fischer, 1942). No recent radiometric dating exists. Recalculation of ^{235}U-^{207}Pb ages of Miller and Kulp (1963) by Ludwig et al. (1984), provides a well-defined peak at about 201 Ma (limit Permian–Jurassic) for the primary mineralization, which would be 30 Ma younger than the age of the Lower Chinle Formation (with maximum ages of deposition at ca. 234–229 Ma, Dickinson and Gehrels, 2008). This age indicates a moderate sedimentary cover at the time of the primary uranium mineralization, which would imply that the tight packing and detrital grains have sutured surfaces and overgrowths observed in the Chinle sandstone (Lewis and Trimble, 1959) suggesting deeper burial than for the sediments hosting the Beverley deposit, would oc-

cur well after the primary uranium mineralization. Other radiometric ages of the uranium mineralization have been estimated at around 180 Ma by Young (1964), followed by several episodes of remobilization by ground water flow.

2.4 Roll Fronts

Roll front deposits generally occur in large to very large sedimentary basins, filled dominantly with Mesozoic to Ceonozoic siliciclastic sediments. Deposition occurs in continental intermountain, vast foreland, to marginal-marine sedimentary basins. The ore bodies present an arcuate shape with a horizontal color zonation and are developed in highly permeable arkosic sandstones or sands located between two aquitars generally corresponding to mudstone-dominated layers. According to their crescent shape they are generally called roll front deposits. Some deposits may display an elongated tabular shape, when the limbs of the roll become predominant because of the presence of carbonaceous-rich clayey-silty layers intercalated within the sandstone unit (e. g., Kellner deposit in South Texas, Dickinson and Duval, 1977). The flow of infiltrated meteoric water is usually driven by gravity. Uranium is deposited at a redox interface, the roll front, which migrates over time allowing a gradual enrichment of the mineralization. Some of these roll fronts are still active today.

The term roll front is presently kept because beyond its descriptive meaning figuring the crescent shape of the ore bodies, roll front also means a redox barrier between a secondarily oxidized sandstone and a primarily or secondarily reduced sandstone, with a horizontal color zonation, a shape also controlled by the confinement of the roll between two aquitards. The host sandstones are unlithified and range from poorly consolidated to completely unconsolidated. Most uranium deposits of roll front type are hosted in arkosic sandstone of Upper Cretaceous or younger in age, but a few occurrences have been described in older host strata but they generally were formed by the remobilization of older tabular ore (Finch and Davis, 1985). The largest roll-front deposits in the world are located in Kazakhstan, the United States, China, and Mongolia (Dahlkamp, 2009; Finch, 1996). A single roll front have a thickness ranging from less than one meter to tens of meters, but is generally less than 20 m thick. In plan-view, along the same stratigraphic horizon, roll front deposits are typically sinuous and can extend up to several hundreds of kilometers along strike. The width of these deposit ranges from less than a meter to several hundred meters (Dahlkamp, 2009). Roll front deposits can be stacked in several superimposed stratigraphic layers at the same locations, as observed in Kazakhstan.

Two subtypes are distinguished among the roll fronts in the IAEA classification (IAEA, 2018a) according to the origin of the primary reductants involved in uranium deposition: either intrinsic reductant consisting of detrital organic matter, or extrinsic reductant such as reducing fluids (liquid and/or gas) migrated from deeper buried oil/gas reservoirs (e. g., Hall et al., 2017 and references therein). Most of the recent studies show that the organic matter represents only a nutrient for the activity of the bacteria for the reduction of sulfates to dissolved reduced sulfur species (H_2S and HS^-) which are the reductant for uranium (e. g., Bonnetti et al., 2020 and references therein). When an extrinsic reductant is involved a structural control on the occurrence of the roll front deposits predominates (e. g., Adams and Smith, 1981). Conversely to the intrinsic redox control, the reduced sandstone overprint primarily oxidized sandstone each side of the structure along which the reducing fluids have percolated. The distribution of the redox zones can be still more complex when the infiltration of the reduced fluids occur after the formation of a roll front, leading to the re-reduction of oxidized sandstone, making difficult the interpretation of the color zonation during exploration of roll front uranium deposits (Zhang et al., 2019; Adams and Smith, 1981). For example, the uranium deposits in the Oakville Formation, South Texas, USA, are entirely hosted within reduced pyrite-bearing sandstone and they have a tabular shape rather than crescent shape. Goldhaber et al. (1979) have found at least three to possibly four stages of pyritization in the Lamprecht deposit in South Texas. This pyritization has been related to the percolation of hydrogen sulfide from oil deposits, or may even have caused direct deposition of uranium (Eargle and Weeks, 1961).

Another sub-type is represented by roll front uranium deposits in North China (e. g., Yang et al., 2020; Bonnetti et al., 2017) characterized by close spatial relationships between U ore bodies and mafic dykes crosscutting the host sandstone. It is proposed that the dykes may have represented an additional reducing barrier to the primary reduced sandstones hosting the mineralization. In the southern Songliao Basin, the sandstone-hosted U mineralization of the Qianjiadian and Baxingtu deposits was attributed to roll front-type mineralization with tabular to more crescent-shaped ore bodies. These deposits are hosted in fluvial to deltaic sandstones of the Late Cretaceous Yaojia Formation. The sandstones of the Yaojia Formation are dominantly primarily oxidized with locally some remnants of primary reduced sandstones. They were then intruded by a series of mafic dykes of basaltic composition during the Eocene (ca. 50–40 Ma; Yang et al., 2020), which were emplaced before the formation of the U deposits in the basin that occurred during the Oligo–Miocene (ca. 40–10 Ma; Cheng et al., 2020). Although the ore formation was mainly attributed to BSR-mediated processes within the primary reduced sandstones of the Yaojia Formation (Bonnetti et al., 2017), the close spatial relation between mafic intrusions and the U ore bodies, dike-related secondary reduction, and secondary oxidation of the mafic rocks in the Qianjiadian/Baxingtu area suggest that Eocene mafic rocks and their alteration halo in the Songliao Basin may have played a role as a reducing barrier for the U mineralization. The hydrothermal alteration related to the mafic intrusions locally resulted in the secondary reduction of the host sediments mainly characterized by bleached and green-altered sandstones. This alteration characterized by newly precipitated chlorite, epidote, and carbonate as sandstone cement has likely formed a secondary reducing barrier in oxidized sandstones or strengthened the reducing character of the primary reduced sandstones. Moreover, the secondary oxidation of some mafic rocks together with anomalous U contents in the sandstones at and near the contact with the dykes (Yang et al., 2020) also demonstrates the interaction between the mafic intrusions and U-bearing groundwaters in the Songliao Basin. Therefore, even though the U mineralization of the Qianjiadian and Baxingtu

deposits are dominantly of roll front type, part of it may have been directly related to the reducing environment provided by the mafic intrusions.

2.5 Interstratified Sandstone-Lignite-Coal Deposits

This sub-type of uranium deposit stands out among the lignite-coal deposits as defined by the IAEA (2018a, b) by: (i) its location precisely essentially within sandstone layers at the contact or interlayed with lignite or coal strata and (ii) its epigenetic origin. This type of deposit occurs in coal/lignite basins with numerous intercalations of coarse siliciclatic sedimentary layers, which serve as channels for infiltration of oxidizing U-bearing water. The deposits directly hosted within lignite or coal horizons in which the uranium mineralization is generally syngenetic and has no relation with sandstones are not incorporated in this category.

Interstratified sandstone-lignite-coal deposits uranium deposits are known in Palaeozoic, Mesozoic and Cenozoic coalfields all over the world (Seredin and Finkelman, 2008). The highest uranium resources occur in Mesozoic to Cenozoic basins. The deposits form in the marginal parts of coal-bearing basins, where infiltration of meteoric waters is possible. The deposits usually consist of a series of wide ore lenses (1 to 15 km long, 0.1 to 2 km wide, and generally 0.1–0.5 m thick, rarely exceeding 1 – 2 m) occurring at the contacts between oxidized sandstones and lignite or coal beds. Russian geologists distinguish two types of epigenetic sandstone-lignite-coal deposits according to the mode of water circulation: (i) direct infiltration of meteoric water (ground-infiltration of unconfined water of Maksimova and Shmariovich, 1993) and (ii) infiltration from formation waters (ground-infiltration of unconfined water of Maksimova and Shmariovich, 1993). Water infiltration is favored when the sedimentation in the basin is followed by weak uplift of the region. Each deposit sub-type is characterized by different shapes and location in the lignite-coal sequences.

The first sub-type, illustrated by the Nizhne Iliskoye deposit (Kazakhstan) or the South Dakota deposits (USA), occurs in monoclinally dipping Jurassic lignite beds and the mineralization is located above these beds. The Nizhne Iliskoye deposit consists of 48 lenticular ore bodies occurring along a 40 km long and 100–2 000 m wide zone. They are restricted to the upper 2 m from the lignite seam. The grade of the ore bodies varies from 0.05% to 2% U, but with an average grade of 0.1% U. Mo, ±Ag, ±Re are associated to uranium. Most of the uranium is adsorbed onto carbonaceous matter and occur as pitchblende and coffinite. The Nizhne Iliskoye deposit occurrs along a redox front between oxidized sandstone and the upper part of the reduced lignite beds according to the geologic cross section provided by Fig. 15 of Seredin and Finkelman (2008).

The second sub-type occurs as classical roll fronts in sandstone with disseminated organic matter, or as elongated lenses within sand horizons devoid of detrital plants parallel to the contact with the lignite layers. The reductant is within the sandstone in the case of the roll front, whereas the redox front is located between the sandstone and the lignite horizon in the case of the elongated lenses, both at the base and to the roof of the sandstone (according to Fig. 16 of Seredin and Finkelman, 2008). However, the largest deposit (Koldzhatsk with 37 000 t U) presents uranium mineralization in both situations: (i) between an oxidized sandstone and the top of a coal layer and (ii) as roll front between coal layers. The deposit is 16 km long and 7 km wide and the ore bodies are associated with three lignite and four sandstone horizons (Kislyakov and Shchetochkin, 2000).

Another subtype of interstratified sandstone-lignite-coal deposits with a tectono-lithologic control can be defined when the uranium mineralization results from infiltration of hydrothermal fluids along faults into the sedimentary layers (exfiltration type of Seredin and Finkelman, 2008). For example, in the Tkhongchong basin in North Korea, the mineralization consists of lens-shaped ore-bodies extending over several tens of meters and up to 5–6 m thick, with average U contents of 600 ppm–800 ppm (Sozinov, 1966). The location of the mineralization is controlled by faults bounding a granitic horst in the central part of the basin and lithostratigraphic horizons with sandstone and coal layer intercalations. The ore bodies occur in basal conglomerates and sandstones with lignite lenses covered by Miocene coal-bearing sediments. The grade of the uranium mineralization increases towards the faults. The hydrothermal fluids are related to an episode of volcanic activity. A similar interpretation is proposed for uranium mineralization in coal beds interstratified in a tuffaceous-sedimentary sequence filling the northern block of the Streltsovska caldera in Transbaikalia (Mashkovtsev et al., 1995). U contents are elevated in coal beds and underlying sandstones and tuffs.

On the contrary the Ambassador polymetallic uranium deposit (Western Australia) (Douglas et al., 2011) despite being hosted within fluvial palaeochannels, is not attributed to the interstratified sandstone-lignite-coal deposit type, because the potentially economic mineralization is entirely contained within the top 1–2 m of lignite seams intercalated with sandstones and was precipitated syngenetically with organic matter.

3 DIAGENETIC HYDROTHERMAL SYSTEMS

Unlike deposits of the preceding group, diagenetic hydrothermal uranium deposits involve the implication of a hot and saline diagenetic brine (70 to 250 °C, 10 wt.% to 35 wt.% eq. NaCl) (e. g., Cuney and Kyser, 2015; Cuney, 2014, 2011; Hoeve and Quirt, 1987). The temperature of the fluid may be in equilibrium or in disequilibrium with the enclosing rocks according to the type of deposit. Some authors have considered that some of the deposits included in this section, such as the tabular deposits were formed at low temperature (e.g., Northrop et al., 1990, for tabular deposits), but these estimations were empirical, and more recent data on temperature estimation of the fluids in these deposits give values of about 100 °C as discussed below. Five sub-types can be distinguished according to the salinity and the temperature of the brine, as well as the location of the redox interface and their depositional or structural environments.

3.1 Intraformational Redox Control

The reducing agent of the uranyl-bearing solutions is present within the sandstone, as dispersed detrital organic matter inherited from land plants, or as migrated humates, or as fluids

deriving from deeper-seated oil/gas reservoirs. This deposit sub-type can be further subdivided in three categories according to the importance of the structural control on the development of the mineralization:

3.1.1 Tabular deposits

They are transitional with the syn-sedimentary deposits, because U may begin to precipitate shortly after sedimentation, but dominantly during diagenesis. This deposit category mainly corresponds to previously name tabular deposits (IAEA, 2018a) from which we distinguished the deposits presenting an important structural control. In tabular deposits, the ore bodies are originally subhorizontal and peneconcordant with the sedimentary bedding and occur within reduced coarse sandstone layers intercalated between weakly permeable clay-rich horizons. However, these tabular deposits may present some complexities, with a structural control which appears in the remobilized part of these deposits, the so called "stacked ores" trapped along tectonic structures, or with the development of roll fronts which may be occasionally a primary features, but more commonly appear to result from the recent infiltration of meteoric fluids (McLemore, 2010). In the present contribution, tabular deposits regroup the formerly distinguished by IAEA (2018a) as continental fluvial deposits, U associated with extrinsic humate typically represented by the Grants district (USA) and continental fluvial vanadium-uranium deposits, typically represented by the Salt Wash-type (USA) because recent syntheses (Barton, 2018; Sanford, 1992) show that most of their characteristics and genetic conditions are very similar.

The depositional environment corresponds to unconfined amalgamated sandy meander-belt (ASMB) deposited across a semi-arid landscape for the Salt Wash sandstone in Colorado (Robbins, 2009). The major source of U and other elements (Mo, Zr) is commonly represented by volcanic ash within the sandstones. Uranium is generally leached by brine under oxidizing and slightly acidic conditions, but interaction with volcanic ashes increases the alkalinity of the fluid. In tabular deposits from the Morrison Jurassic Formation in Colorado (Shawe, 2011) the sandstone is lithified, quartz grains present evidence of pressure solution and variably developed overgrowths suggesting deeper burial of the sediments compared to the sandstone units hosting roll front uranium deposits. Pressure solution becomes significant beyond a burial depth of about 2.5 km (Ramm, 1992). In the sandstone, feldspars represent generally less than 10 vol% of the rock. In the cement, chlorite is frequently rich in vanadium, and associated with interstratified clay minerals, illite and kaolinite. The tabular ore bodies are completely enclosed by reduced, pyrite-bearing sandstone; they are not localized along redox boundaries. No oxidation of pyrite is observed. From these observations Granger and Warren (1979) suggest that unlike roll front deposits, the uranium-bearing fluid in tabular deposits were devoid of free oxygen. Another important parameter may be the difference in the type of complexation of uranyl ions. In infiltrated meteoric water, uranyl-carbonates are probably the main species in solution, and carbonates are known to enhance pyrite oxidation (Caldeira et al., 2010). Whereas, in tabular deposits, the ore fluid involves a higher temperature (70 to 110 °C for the Colorado Plateau district, Shawe, 2011; Meunier, 1994; Meunier et al., 1987) chloride diagenetic brine (0 to 14 wt.% equiv. NaCl for the Colorado Plateau district, Meunier, 1994), in which uranyl ions may be associated with other type of complexes (S, Cl) which may be less reactive with iron sulfides and organic matter, preventing the formation of a distinct redox front. If this brine is associated with the mineralization process, its temperature is not compatible with an activity of sulfate reducing bacteria supported by the presence of framboidal pyrite and the very negative values of $\delta^{34}S$ of the sulphides in mineralized samples (e.g., Northrop et al., 1990). However, it is possible that these sulphides and associated bacterial activity may have occurred during an early diagenetic stage, before the circulation of the hot diagenetic brines. Framboidal pyrite texture may survive low-grade metamorphism (e.g., Hellerschmidt-Alber, 2008 in the Forstau deposit, Austria). In addition, tosudite has been identified in the Tidwell Member, just below the mineralized section of the Salt Wash Member of the Morrison Formation (Northrop et al., 1990). The temperature of tosudite crystallization has been estimated between 100 and 200 °C from the data on the thermal stability of tosudite in the literature (Beaufort et al., 2015).

The lack of any obvious geologic feature controlling at the local scale the striking tabular geometry of these deposits has led several authors for the ore deposits of the Morrison Formation (e.g., Northrop et al., 1990, and references therein) to propose a model involving a stable interface between two density-stratified fluids, a brine and a meteoric fluid. However, the most recent synthesis (Barton et al., 2018), suggests that migrated hydrocarbons are likely responsible for the reduction of the uranyl-bearing solutions. Ludwig et al. (1984) propose however an age of about 132 Ma for the primary uranium mineralization of the Ambrosia Lake district hosted in the Morrison Formation, an age close to that of the deposition of the Late Jurassic host rock. Although these results seem to be consistent with the Rb/Sr age on ore-stage chlorite of Brookins (1980), suggesting a primary mineralization age at 139±24 Ma in the same district, they are in contradiction with the oldest possible migration age of reducing fluids derived from an oil reservoir in the area, estimated from modelled age of oil maturation, at less than 100 Ma (Nuccio and Condon, 2000). A recent contribution, on the small JD6 uranium mine (with a resource of about 50 t U), from the Uravan belt in Nebraska, gives U-Pb ages with four stages of uranium deposition, the earliest one is dated at 34±5 Ma on coffinite associated with non-biogenic pyrite (Meek, 2014). It clearly appears that further research is needed to clarify the nature of the mineralizing fluids, to better evaluate the relative role of detrital organic matter versus migrated reducing fluids, the mechanism of uranium reduction, and the age of the primary uranium deposition for this type of deposit.

More recently, evidences of hydrothermal fluid involvement have been reported in a number of sandstone hosted uranium deposits from China, such as the Hangjinqi uranium deposit in the Northern Ordos Basin (Zhang et al., 2017), the Qianjiadian uranium deposit in the Songliao Basin (Jia et al., 2020; Rong et al., 2020, 2019), and Tamusu uranium deposit, Bayingobi Basin (Zhang et al., 2019). The Hangjinqi uranium

deposit represents an interesting example of a primary low temperature mineralization followed several tens of million years later by a uranium mineralization associated with hot and saline fluids (120–180 °C and 8.00%–16.34% eq. wt.% NaCl) (Zhang et al., 2017). However, it is not specified whether the hydrothermal stage represents only a reworking of the primary low temperature mineralization or if it contributes to an important part of the uranium resource in the deposit. Nevertheless, the hydrothermal uranium stage dated at 39±2 Ma by Zhang et al. (2017) likely contributed in local enrichment as well as the preservation of the primary reduced U ore, which was favored by the Eocene (~50–40 Ma) crustal extension and related mafic intrusions in northeast China (Yang et al., 2020). On the contrary in the case of the Tamusu uranium deposit, Zhang et al. (2019) show that the hydrothermal diagenetic fluid is responsible for the formation of the high-grade mineralisation. For the Qianjiadian uranium deposit, the formation of the high-grade mineralization is attributed to the thermal effect of the intrusion of diabase dykes (Jia et al., 2020; Rong et al., 2020, 2019). However, a more recent study (Yang et al., 2020) constrains the emplacement of the basic dykes by zircon U-Pb isotopic dating (between 51 and 40 Ma) prior to the main stage of uranium mineralization (Zhao et al., 2018). Therefore, if the mafic rocks have played a role as a reducing agent in the genesis of the high grade U ore, as suggested by the occurrence of the U ore bodies close to the mafic dikes, the high temperature fluids do not seem to be related to the ore forming processes.

3.1.2 Tectonolithologic deposits

The ore bodies are controlled not only by the host lithology-permeable palaeochannels rich in reducing organic compounds as in the preceding deposit types-but also by tectonic structures. Typical examples are the deposits from the Arlit-Akouta district in Niger (Pagel et al., 2005) and the Lodève Basin, from southern France (Mathis et al., 1990; Comte et al., 1985).

In Niger the location of the deposits and paleochannels are controlled by the Arlit-Inazawa lineament and associated structures, but the mineralization is stratabound (Gerbaud, 2006). Most of the deposits are hosted in the Pennsylvanian or Jurassic Formations. Roll front type structures are particularly obvious in the Akouta deposit, but result from uranium remobilization from primary mineralization by later infiltration of meteoric fluids (Cazoulat, 1985), probably during the uplift of the basin. In the Lodève deposit, the uranium mineralization occurs both within organic matter-rich sedimentary layers, with a possible primary uranium preconcentration (Lancelot and Vella, 1989), and along tectonic structures in association with migrated bitumens (Martin, 1992).

The Permo-Pennsylvanian Lodève Basin is an intermontane basin with up to 3 000 m of sediments deposited in a fluvial-alluvial to lacustrine setting. However recent interpretations propose that the stratigraphic relationships in the Lodève Basin may be the product of a progradational deposition on a distributive fluvial system (DFS) (Weismann et al., 2013). A DFS is defined as ‘the deposit of a fluvial system which in planform displays a radial, distributive channel pattern’ (Hartley et al., 2010). The main mineralization is localized in the Lower Autunian and more specifically in the Loiras and Mas d’Alary layers. They consist of alternating 0.5 to 2 m thick strata, each comprising three types of lithology: fine-grained sandstone at the bottom deposited in continental flood plains, overlain by carbon matter-rich silt and shales, and finally pelites at the top deposited in lagoonal environments. Twenty layers of centimeter-to-decimeter-thick cinerites are interbedded within the Autunian shales. Another particularity of this deposit is that the organic matter is of mixed origin, with most of it deriving from planctonic organisms and algae with a small proportion of detrital plants. The fluids present in quartz and dolomite veins within the deposit have the characteristics of a diagenetic brine with varied salinities (3 wt.%–14 wt.% eq. NaCl) and homogenization temperatures (130–250 °C), but temperatures up to 300 °C were reported (Mendez Santizo et al., 1991; Landais and Connan, 1986). The new formation of K-feldspar indicates that the fluids were alkaline.

In the Arlit-Akouta district in Niger the depositional environment of the mineralized sandstone is essentially fluvio-deltaic (Valsardieu, 1971). At a more detailed scale, the mineralization is preferentially located along bottom and basal fore set layers of palaeochannels where carbon (organic) matter is preferably accumulated and replaced by pyrite (Sanguinetti et al., 1982). The sandstone is lithified with quartz grains presenting evidence of pressure solution and variably developed overgrowths suggesting deep burial of the sediments. In the ore deposits, the temperature of the fluids (85 to 175 °C) estimated from chlorite composition and fluid inclusion studies (Mamadou, 2016; Mamadou et al., 2016; Forbes, 1988), and their salinities correspond to those of a diagenetic brine (3 wt.% to 22 wt.% eq. NaCl). The fluids were alkaline, as attested by the abundance of analcime and carbonate in the sediments, and the new formation of albite. The location of the deposits is controlled at the reginal scale by the Arlit-Inazaoua lineament and the paleochannels are controlled by associated diverging structures (Gerbeaud, 2006). In this area, the structural control of the mineralization is the most evident in the newly discovered Dasa uranium deposit about 80 km south of the Arlit district, which is located in a N70 trending graben structure (Sani et al., 2020).

The major source of U is represented by volcanic ash present within the sandstones in the Arlit-Akouta district (Forbes et al., 1984) as well as in the Lodève deposit (Ahamdach et al., 1993). However the surrounding U-rich granitic and or volcanic rocks have certainly also contributed to the early uranium enrichment of the organic matter-rich sediments during their deposition. Regarding uranium deposition, its reduction by the intrinsic organic matter is the favored hypothesis for the deposits in the Arlit-Akouta district, although migrated hydrocarbons have been recently evidenced in these deposits (Salze et al., 2018). Concerning Lodève, the control of the uranium mineralization by migrated bitumen is clear for the structurally controlled mineralization in addition to the intrinsic organic matter control for the stratabound mineralization.

3.1.3 Diagenetic-hydrothermal karst

Although this type of deposit is not hosted in sandstone, it

is proposed to integrate it to the sandstone type uranium deposit classification because it occurs in the same sedimentary basin as the valley-confined amalgamated sandy meander-belts and the tabular deposits from Colorado, and the fluids described in the ore bodies are diagenetic brines similar to those observed in the tabular or tectono-lithologic deposits described above.

They are generally referred to as solution collapse breccia pipes (IAEA, 2018a). They are nearly only known in the Grand Canyon region in the Colorado Plateau, USA, but similar occurrences have been reported in China. They form almost vertical cylindrical pipes of 30 to 175 m wide located in the Upper Carboniferous to Triassic flatlying sediments (Wenrich and Titley, 2008). Karstification developed in the Mississippian Redwall Limestone mainly along and at fracture intersections. Overlying sedimentary formations have collapsed up to a distance of 1 000 m from the karst cavities. Several thousands of pipes have been identified but only about 100 of them are mineralized. Ore grades are elevated (0.4% to 1% U), but resources are relatively small (some hundreds to 1 500 t U). Pitchblende is the main U mineral, and is associated with a variety of Cu, Zn, Pb sulphides and arsenides and locally bitumen disseminated in the matrix of the pipe filling breccias and as fillings of minor fractures. The fluids trapped in sphalerite, dolomite and calcite are typical diagenetic brines, infiltrated from deeper part of the basin, with homogenization temperatures of 80–173 °C and salinities of 4 wt.%–17 wt.% equiv. NaCl (Wenrich and Titley, 2008). All these characteristics are quite similar to those of Mississippi Valley-type deposits. Interestingly, the U-oxides from several breccia pipe deposits (Pigeon, Kanab N, and Hack 2) display similar chemistry and REE patterns (Wenrich et al., 2018; Lach, 2012), to U-oxides from unconformity-related uranium deposits (Mercadier et al., 2011), which genesis is also related to the circulation of diagenetic brines. The reductants is not very well defined but may be represented by migrated hydrocarbons preserved as bitumens in some of the pipes (Landais, 1986). Two mineralization events have been dated at 260 and 200 Ma (Ludwig and Simmons, 1992), implying that the brine would have circulated much earlier than the one associated with the valley-confined amalgamated sandy meander-belts hosted in the Triassic Chinle Formation and the tabular deposits of the Jurassic Morrison Formation also occurring in the Colorado Plateau region. However, thermal modelling of the Permian Toroweap Formation associated with uranium deposits in Colorado Plateau breccia pipes, gives a maximum age of 120±10 Ma for the migration of the hydrocarbons in the pipe (Landais, 1993), which would be similar to some of the ages obtained by Ludwig et al. (1984) for the primary uranium mineralization of the tabular deposits of the Ambrosia Lake district at about 132 Ma.

In South China, Devonian–Carboniferous carbonate strata host several uranium deposits (Sanbaqi, Sanqilinyi, and Saqisan), with characteristics similar to those of the Colorado Plateau breccia pipes (Min et al., 2002). For example, the Saqisan uranium deposit occurs in solution collapse breccias as well as in solute on-fault breccias with a mineralization consisting of pitchblende, coffinite and Fe-, Cu-, Zn-, Pb-, and Ni-sulphides. The breccia matrix is composed of limestone clasts, clays and organic matter. An early uranium mineralization associated with organic matter synchronous with karst formation, is later enriched during the percolation of a saline basinal brine at 110–251 °C.

3.2 Interformational Redox Control

The reducing interface is located between the top of an oxidized sandstone formation and an oil generating black shale formation as exemplified by the deposits of the Early Proterozoic Franceville Basin in Gabon (Gauthier-Lafaye, 1986). This example shows that uranium deposits hosted in sandstone occured well before the apparition of the land plants, by the creation of reducing conditions in the sandstone through the migration of hydrocarbons generated in marine sediments. The Franceville basin is filled with a 4 to 5 km thick, unfolded and unmetamorphosed, sedimentary succession deposited at about 2.1 Ga.

The basal FA Formation (500 – 1 000 m thick) is mainly composed of conglomerates and fine- to coarse-grained red sandstones, deposited in a fluvial to deltaic environment (Weber, 1968). The FA sandstone being of Proterozoic age, synsedimentary organic matter was absent, whereas the shales of the overlying FB formation deposited in marine environment are very rich in organic matter. All uranium deposits of the Franceville basin (e. g., Oklo, Mounana, Okelonbondo) occur in the upper part of the FA formation, in the vicinity of the contact with the FB black shales (Gauthier-Lafaye, 1986). Gancarz (1977) has dated uranium deposition by U-Pb isotopes at 2.05± 0.03 Ga. The development of the mineralization is controlled both by the stratigraphy and the tectonic structures. The fluids presumed to be associated with the ore forming processes have the same characteristics as those of unconformity-related deposits: maximal burial temperature of about 200 °C and 1 kbar, and with high salinities (28.7 wt.% NaCl to 30 wt.% $CaCl_2$ eq.) (Mathieu et al., 2000). The main uranium source is believed to come from the alteration of the detrital monazites particularly abundant in the FA formation (Cuney and Mathieu, 2000). It has been calculated that the amount of U liberated from monazite alteration by the oxidizing diagenetic brines was largely sufficient to account for all the uranium deposits of the Franceville basin (27.635 t U at 0.38%). The reduction of uranium is controlled by the hydrocarbons generated by the thermal maturation of the marine organic matter of the FB black shales, which have migrated in the permeable sandstone in the upper part of the FA Formation, and have mixed with the oxidizing uranium-bearing diagenetic brines (Lecomte et al., 2020). The hydrocarbons have migrated thanks to the development of longitudinal normal faults (Ndongo et al., 2016), and hydrofracturing of highly silicified sandstones. Hydrofracturing was related to the development of overpressures in undercompacted zones, and have favored fluid circulation and mixing (Gauthier-Lafaye and Weber, 1989). The main generation of uranium oxides in the deposits of the Oklo district displays similar chemistry and REE patterns (Lecomte et al., 2020) to the U-oxides from unconformity-related uranium deposits (Mercadier et al., 2011) and also U-oxides from the Pigeon, Kanab N, and Hack 2 breccia pipe deposits (Wenrich et al., 2018; Lach, 2012).

The Mountain Lake deposit hosted in the Paleoproterozoic Hornby Bay Basin, in the Bear Structural Province (Canada), presents a location in the basin similar to that of the Oklo district uranium deposits. It is located in sandstone of the LeRoux Formation, close to its upper boundary with black shales of the Fort Confidence Formation. Dayboll et al. (2010) propose that downward-moving hydrocarbons, originating from the overpressured shales of the Fort Confidence Formation, represent the reducing agent for the reduction of uranium. They classify this deposit as a tabular, sandstone-hosted deposit, despite the strong dissimilarities with the typical tabular deposits as originally defined in Colorado. This example shows once again that a purely descriptive classification of uranium deposits can be misleading.

3.3 Basement/Basin Redox Control

They are usually referred to unconformity-related deposits due to their location close to surface of unconformity between an undeformed siliciclastic sedimentary cover and a metamorphic basement. These deposits are integrated in the classification of sandstone type deposits because the sandstone represents the reservoir of the ore forming fluids and at least a part of the uranium forming the deposits, even if some of the deposits are not hosted in the sandstone, but in the basement or straddle the unconformity. The basement is usually represented by Archaean granitic domes rimmed by metamorphosed Palaeoproterozoic U-rich epicontinental sediments, and intruded by granitic/pegmatic bodies. The basal formation in these basins consists of continental fluvial, aeolian to marginal marine, oxidized, sandstone with minor siltstone which deposition begins at about 1 750 Ma (Jefferson et al., 2007). In the heavily mineralized basins, the sandstone is very mature, comprising well-rounded detrital quartz with generally well-developed overgrowths, minor clay cement consisting mainly of kaolinite, and feldspars are generally absent. The mineralization is essentially controlled by tectonic structures, commonly corresponding to reverse faulting. These faults have a long tectonic history, from pre- to post-basin, and are deeply rooted in the basement in graphitic schists (referred also as graphitic conductor). Along these structures, quartz dissolution in both basement and basin is an important phenomenon that provides most of the space for the deposition of the uranium mineralization (Lorilleux et al., 2002). When silicified, the sandstones are brecciated (Le Carlier et al., 2009). The two major provinces hosting basement/basin redox-controlled deposits are the Athabasca, Saskatchewan in Canada and the East Alligator River, Northern Territory in Australia, uranium Provinces. Other basins that share some of the characteristics of the Proterozoic Athabasca and McArthur basins and hosting basement/basin redox-controlled deposits are known the Proterozoic basins of Pasha Ladoga in Karelia, Russia, with the Karku deposit (Velichkin et al., 2005), Thelon in Nunavut (Renac et al., 2002), Otish in Northern Québec (Beyer et al., 2012, both in Canada, and the metamorphosed Coolbro Sandstone in Australia, with the Kintyre deposit (Hanly, 2005). A complete review of the basement/basin redox-controlled uranium deposits is available in IAEA (2018a). A thorough discussion concerning the deposits that have been improperly attributed to this deposit type is also provided.

Possible U sources of basement/basin redox-controlled deposits are some lithologies from the basement and the sandstone cover. Archaean rocks underlying the Athabasca Basin are mainly composed of U-poor tonalites and cannot have represented a U source, a few are slightly enriched in uranium, but high-K-Th-U Archaean granites do exist (Nanambu Complex) in the Northern Territory. These Archaean domes in both provinces are rimmed with Palaeoproterozoic metasediments made of epicontinental clastic to chemical deposits. Graphitic schists representing former black shales deposited during the Shunga event just after the Great Oxygenation Event are enriched in uranium and represent probably the dominant source of U and associated elements (Partin et al., 2013; Cuney, 2010). Many other additional potential uranium sources are present especially in the basement of the Athabasca Basin. Meta-arkoses and calcsilicates, as well as pegmatoids and leucogranites derived by anatexis of the Palaeoproterozoic meta-sediments, are rich in uranium and contain uraninite, which represents a particularly easily leachable U source (Mercadier et al., 2013; Annesley et al., 2003; Parslow and Thomas, 1982). Palaeoproterozoic U-Th-rich high-K calc-alkaline granitoids, and the late Hudsonian U deposits of the Beaverlodge-Gunnar district may also represent significant U sources.

The sandstone cover may have represented an additional or a main U source (Fayek and Kyser, 1997). However, the mean U content of the conglomeratic and sandstone formations in the Athabasca and McArthur basins is about 1 ppm, and predominantly hosted in zircon. Only the alteration of monazite has represented a potential notable U source, as already discussed above for the uranium deposits of the Franceville basin, Gabon (Cuney and Mathieu, 2000; Hecht and Cuney, 2000). However, a significant part of the U liberated by monazite alteration was trapped in Fe-Ti oxides and in altered zircons (up to to several thousand ppm), but not leached out from zircon as proposed by Fayek and Kyser (1997). In contrast with these observations, Chi et al. (2019) propose, from the study of fluid inclusions in the diagenetic overgrowths of detrital quartz from the Athabasca sandstone, that the early diagenetic fluids were already relatively rich in uranium up to a few tens of ppm.

Uranium solubility was favored by the high temperature (120–200 °C), f_{O_2} and chlorinity (25 wt.%–35 wt.% eq. NaCl) and low pH of the basinal diagenetic brines derived from evaporation of seawater at surface (Richard et al., 2011; Derome et al., 2005, 2003). The high temperature is the result of a deep burial of the sandstone (4 to 5 km), the high f_{O_2} resulted from the lack of detrital or migrated organic matter in Palaeoproterozoic continental sandstones, the high chlorinity from the high degree of evaporation leading to evaporates in upper horizons of the basin, and the low pH from the lack of detrital feldspar and the presence of a quartz+kaolinite±illite paragenesis in the cement of the sandstone. The efficiency of these brines for U transport has been confirmed by the laser ablation ICP-MS analyses, which have revealed that the brines have U concentrations reaching several hundreds of ppm (Richard et al., 2012), the richest U concentrations in natural fluids known so far. An alternative hypothesis considers a shallow burial of the Athabasca sandstone and that the high temperatures were resulting

from an anomalous heat flow induced by the intrusion at depth of basic magmas (Chi et al., 2018).

The oldest uranium mineralization age in the Athabasca Basin district is at ca. 1 590 Ma, from U-Pb dating of U-oxides and ^{40}Ar-^{39}Ar dating of syn-ore illite, for both sandstone- and basement-hosted deposits (Alexandre et al., 2009). In Australia, an age about 1 680 Ma has been determined for the main diagenetic-hydrothermal uranium mineralization (Skirrow et al., 2016). However, it is still uncertain if all the U has been deposited during a single event or if accretion of multiple stages of U deposition have occurred, as the uranium oxides and clays are marked by an extremely large dispersion of measured ages (from 1.7–1.5 Ga to present time)

To explain uranium reduction, as well as the source of boron and magnesium in the alteration haloes and of the metals (Ni, Cu, Co, Zn, Au) in the polymetallic deposits, a reduced fluid derived from the basement has been proposed by various authors (e.g., Dargent et al., 2015; Bray et al., 1988; Hoeve and Quirt, 1987). However, direct evidences for the mixing of a basement derived reduced fluid with the basinal brines are still very weak. The deposition of the Ni-Co-Cu-As-S stage at Cigar Lake U deposit (Athabasca Basin) is moreover temporally disconnected from the first stage of U deposition and considered to be related to the McKenzie dykes emplacement at 1.27 Ga (Chernonozhkin et al., 2020). Other hypotheses have been proposed for the reduction of uranyl ions (see Kyser and Cuney, 2015 for a synthesis).

3.4 Basin/Basement Redox Control

The definition of this type of deposits is based on the fact that the conceivable reductants are located in the basin and are not available in the basement. The redox zonation is inverted relative to the basement/basin type discussed just above. Such deposits have been described in the northern part of the Proterozoic Cuddapah Basin located in the eastern Dharwar Craton in India (Verma et al., 2009). Typical examples of this type are the Chitrial (5 000 to 10 000 t U at 0.05% to 0.10% U) and Koppunuru (700 t U at 0.07% U) deposits associated to the Srisailam and Palnad sub-basins. The mineralization occurs as thin, elongated sheets parallel to an Archaean unconformity surface either mostly at the top of the Archean U-Th-rich granitic basement in the Chitrial deposit, or as horizontal lenses concordant with the sedimentary bedding in the Banganapalle Formation above the unconformity with minor mineralization in the basement for the Koppunuru deposit. The Banganapalle Formation consists of a basal conglomerate, quartz arenites with intercalation of carbonaceous shales.

A chlorite alteration is essentially developed in the upper part of the granite and rarely in sediments, and illite occurs both in the granite and the arkosic quartzite. Organic matter and pyrite commonly occur with the uranium mineralization, which suggests that they may have been involved in the reduction of uranium. The fluid inclusions associated to these deposits have the characteristics of diagenetic fluids (1.9 wt.% to 23.2 wt.% NaCl eq.; 82 to 226 °C) (Thomas et al., 2014). The large salinity variation associated with the range of homogenization temperatures of the fluid inclusions has been interpreted by Thomas et al. (2014) as a mixing between a low saline fluid which is attributed to a basinal brine, and an evolved brine resulting from hydrothermal alteration. However, another interpretation is preferred. The brines probably derive from deeper part of the Cuddapah Basin, where the temperatures were higher, and have migrated to the marginal part of the basin following the unconformity contact as observed in other basins (Boiron et al., 2010). The source of the uranium is most probably the U-Th-rich granites from the basement. The reductants are probably the organic matter derived from the pyritic black shale layers.

3.5 Mafic Intrusion Redox Control

The uranium mineralization occurs in the vicinity of or within mafic dykes and sills that crosscut or are concordant with Proterozoic sandstone strata. For example the Red Tree deposit hosted in the McArthur Basin, Westmoreland District, Australia, is essentially stratabound within the sandstones and parallel to the lithological contacts with dolerite sills. The McArthur Basin was filled by several kilometers of siliciclastics, carbonates, and volcanic tuffs, between 1 800 and 1 600 Ma. The Westmoreland Conglomerate overlay the felsic Cliffdale Volcanics, both representing the basal part of the Tawallah Group. The Cliffdale Volcanics comprise ignimbritic tuffs and rhyolitic lavas (Orth, 2010). The Westmoreland Conglomerate is mainly composed of conglomerates and sandstones reaching a thickness of up to 1 800 m, representing proximal fluvial deposits with debris flows, alluvial fans, and braided river systems that are overlain by well-sorted sandstones (Ahmad and Wygralak, 1989). The Conglomerate is covered by the mafic Seigal Volcanics, followed by dolomite, sandstone, felsic and mafic volcanic rocks of the upper part of the Tawallah Group. The Westmoreland Conglomerate is highly immature and poorly sorted, and consists of detrital cobbles and coarse sand grains consisting in reworked quartz veins, cherts, and clasts of felsic to mafic volcanic rocks and feldspar. The conglomerate is the host of most of the uranium mineralization. After deposition of these sediments, the Isan Orogeny produced an east-west shortening, associated with low-temperature metamorphism followed by strike slip faulting (Garven, 1999). The age of peak metamorphism for the Isan orogeny is estimated at ca 1 600 – 1 580 Ma (Giles and Nutman, 2002). The oldest ages were obtained on the Redtree U-oxides, with $^{207}Pb/^{206}Pb$ ages of 1 606±80 and 1 655±83 Ma (Polito et al., 2005). The oldest age is similar to the 1 680±21 Ma $^{40}Ar/^{39}Ar$ age determined on diagenetic illite from the Westmoreland Conglomerate (Polito et al., 2005) and to the 1 685±65 Ma age determined on apatite associated with U-oxides from the Junnagunna deposit (Gigon et al., 2021). Therefore, first stage of U-oxide deposition may have occurred at ca. 1 680 Ma and followed by several episodes of deposition and/or remobilization (Gigon et al., 2021; Polito et al., 2005). The location of the uranium mineralization is not controlled by sedimentology, but by basic dyke and sill intrusions, and by tectonic structures.

For Polito et al. (2005) these deposits share similar mineralogical, geochemical, and age characteristics to that described for the uranium deposits associated to the Kombolgie and Athabasca basins, suggesting that they result from similar genetic processes. In addition, fluid inclusions studies by Mernagh and

Wygralak (2011) have identified NaCl-rich and $CaCl_2$-rich brines mixed in varying degrees with a low-salinity fluid, as already documented for the basement/basin redox controlled deposits related in the North of the McArthur Basin. Despite these similarities, the physical and chemical conditions that have prevailed during the formation of the deposits differed between the two districts (Gigon et al., 2021). The temperature estimated from chlorite thermometry (>300 °C; Gigon, 2019) and fluids inclusions (99 – 380 °C; Mernagh and Wygralak, 2011) were significantly higher than in the deposits related to the Kombolgie sub-basin, for the early U mineralization stages, and the characteristic Mg- and B-alteration paragenesis associated to the basement/basin redox controlled U deposits is lacking in the Westmoreland district. Alumino-phosphate-sulphate minerals are also absent. In addition, most minor and trace elements, including REE, are in significantly higher concentrations in the uranium oxides from the Westmoreland area, which may result from the higher temperature of genesis of these deposits (Gigon et al., 2021; Gigon, 2019). The typical bell-shape of the REE patterns of uranium oxides of the basement/basin redox controlled U deposits is also lacking, but these patterns are similar to those of the metamorphic-hydrothermal deposits of the Otish Basin (Gigon, 2019). All these data points to specific ore-forming processes for this type of basin-related U deposits in the Westmoreland district. The Matoush deposit in the Otish Basin, Canada, (Alexandre et al., 2015) which occurs along the margins of vertical dykes, represents the closest analogue of the uranium deposits of the Westmoreland district.

Uranium deposits with mafic intrusion redox control are small to medium (300–10 000 t) in size and have low to medium grades (0.05%–0.40%) (IAEA, 2018b).

4 SEDIMENTARY-VOLCANIC SYSTEMS

Volcanic-sedimentary deposits consist of carbonaceous fluvial/alluvial or lacustrine sandstone with a more or less significant trachytic-rhyolitic volcanic tuff contribution. Low grade (50 ppm–200 ppm U), peneconcordant and extensive uranium accumulations associated with anomalous contents of V, Mo, Li, F, B, Cu and Ni encompass zones with higher grade mineralization. There is in fact a complete transition between sandstone from hardly detectable to dominant volcanic contribution. In many sandstone uranium districts, the volcanic contribution has been mostly identified from repeated cinerite layers within the sedimentary succession, but distinct from the mineralized sandstone horizons, such as in the roll front district of Wyoming, USA (Zielinski, 1983) or the Lodève district in France (Mathis et al., 1990). In the Sierra Pintada district in Argentina (Kleiman, 1999) with a resource of 11 000 t U at a grade of 0.1% U, or the Anderson Mine in the USA (Mueller and Hallbach, 1983) with a resource of 11 000 t at a grade of about 300 ppm U, the volcanic contribution becomes predominant in the mineralized sandstone horizons themselves. More discrete volcanic contribution can be evidenced by the presence of glass shards, embayed quartz texture, pumice stones. However advanced diagenesis may destroy these evidences. An interesting identification of a volcanic contribution can be made by studying magmatic inclusion in volcanic-detrital quartz from the sandstone (Ahamdach et al., 1993; Forbes et al., 1984), that allows to get the chemistry of the melts and in particular their initial uranium contents.

The Sierra Pintada uranium district (Kleiman, 1999), San Rafael, Mendoza, Argentina is hosted by Permian sandstones of the Areniscas Atigradas Member belonging to the lower part of the Cochicó Group. The Cochicó Group represents the lower section of the large Choiyoi volcanic province of Chile and Argentina, which emplaced between ~280 and 250 Ma at the western Palaeo-Pacific margin of Gondwana. The Cochicó Group is a succession of alluvial fan deposits, of dacitic ignimbrite flows and interbedded aeolian and fluvial sandstones. The mineralized sandstone itself includes a very important pyroclastic material component, as acid plagioclase, quartz, and volcanic lithic fragments. The ignimbrites are crystal rich and are considered the main source for the uranium. The largest occurrence in the district is the Dr Baulíes deposit with reserves close to 6 000 t U. The uranium mineralization displays a tabular shape. Primary uranium minerals are uraninite, coffinite and brannerite. Sulphides, organic matter, chlorite and abundant Fe-Ti minerals are considered as the reducing agents for uranium precipitation.

5 SYNMETAMORPHIC SYSTEMS

Some deposits hosted in sandstone have been formed by high temperature fluids that have characteristics of metamorphic fluids rather than diagenetic brines. This type of deposit is for example illustrated by the uranium mineralization associated with the Paleoproterozoic Otish Basin and particularly the Camie River deposit on which several recent studies are available (Lesbros-Piat-Desvial et al., 2017; Beyer et al., 2012). The Paleoproterozoic Otish Basin is located at the southeastern margin of the Archean Superior Province, Québec, Canada, and is mainly filled with continental clastic sediments of the Otish Supergroup (Genest, 1989). Sedimentation starts with the high-energy fluviatile syn-rift depositional environment of the Indicator Group characterized essentially by greenish clastic fluvial poorly sorted siliciclastic rocks, and evolves towards lower-energy sedimentation of the Peribonca Group consisting of reddish clastic deltaic sedimentary rocks. The Indicator Group comprises the Matoush Formation overlain by the Shikapio Formation. The sedimentation of the Otish Supergroup should be older than the baddeleyite U-Pb ages of the Otish Gabbro dykes and sills that intruded the Otish Supergroup (2 172 – 2 162 Ma) (Hamilton and Buchan, 2016), much older than the Athabasca or McArthur basins hosting basement/basin redox control deposits presented above.

In addition, unlike the Athabasca and McArthur basins, the Otish Basin was subjected to brittle deformation and variable degree of metamorphism (Chown, 1979). The northwestern part of the basin has been subjected to sub-greenschist metamorphic grade restricted to fault zones, while in its southeastern part regional metamorphism increases from greenschist to the amphibolite grade towards the Grenville Front. These events have promoted diagenetic/metamorphic hydrothermal alteration, and U mobilization within the Otish Basin.

More than 30 uranium occurrences are known in the Otish Basin and underlying basement. Four types of deposit have been defined by Gatzweiler (1987) and Höhndorf et al. (1987):

stratiform and vein-type mineralization in the basement, mineralization at the unconformity (Camie River), and vein-type mineralization in the Otish Supergroup sediments at the contact with faulted mafic dykes (e.g., Matoush et al., 2016).

The Camie River deposit is located at the southwestern margin of the Otish Basin. The uraninite and brannerite mineralization occurs in a reverse faulted-contact at the unconformity between the massive sulfide and graphitic schist of the basement and the sedimentary Matoush Formation. The deposit extends from 20 to 50 m above and below the unconformity along the fault (Gatzweiler, 1987; Höhndorf et al., 1987). The deposit has been dated at about 1 724 Ma on uraninite and molybdenite (Lesbros-Piat-Desvial et al., 2017; Beyer et al., 2012). Despite its location at the unconformity, its structural control by reverse faulting, the presence of a polymetallic association and the presence of graphitic schists in the basement, the Camie River deposit presents a series of major differences with basin/basement redox-controlled deposits. The sandstones of the Matoush Formation are reduced and therefore were probably deposited before 2.2 Ga, e.g., before the Great Oxidation Event, this means that no redox contrast between the basin and the basement existed; the sediments of the Matoush Formation are immature with large amounts of detrital feldspars compared to the mature quartzose sandstones of the Athabasca or Kombolgie Basins, indicating more alkaline diagenetic brines in the sandstones in accordance with the observed albitic alteration (Lesbros-Piat-Desvial et al., 2017; Beyer et al., 2012); the early albite cementation of the basal sedimentary sequence at Camie River have occluded its permeability preventing significant fluid flow of the diagenetic fluids within the basin; the temperature of uranium deposition occurred at a much higher than for typical basin/basement redox controlled uranium deposits; the characteristic alteration paragenesis (i. e., sudoite, dravite, APS) is lacking at Camie River and other uranium deposits from the Otish Basin; finally the rare earth element pattern of the Camie River uranium oxides are typical of high temperature, syn-metamorphic uranium mineralization, such as the syn-metamorphic uranium deposits of Mistamisk, Canada (Kish and Cuney, 1982) and of the Lufilian Belt (Eglinger et al., 2013), formed at similar temperatures.

This type of deposit requires a better characterization of the ore forming fluids from fluid inclusion studies. An interesting question is the fact that the Camie River deposit was dated with rather good accuracy at about 1 724 Ma on uraninite and molybedenite (Lesbros-Piat-Desvial et al., 2017 and references therein), with little evidence of the effect of the intense Grenville deformation and metamorphism developed at 1 090–980 Ma (Hynes and Rivers, 2010), only at a few tens of kilometers from these deposits, and the rather strong metamorphic footprint present in the Otish Basin, although the age of this metamorphic event has not been determined.

6 METAMORPHOSED DEPOSITS

This type of deposit represents a mineralization hosted in sandstone, which has been subjected to deformation and metamorphism. These deposits have been deformed and heated up, but without any new uranium supply during the metamorphic event. This type of mineralization has been poorly recognized especially when occurring in terranes with high grade of metamorphism and partial melting. Uranium mineralization in metarkoses appears in continental to epicontinental sediments after the Great Oxygenation event at about 2.0 – 2.3 Ga (Cuney, 2010). Typical examples are those of the Wollaston belt, Northern Saskatchewan, Canada (Parslow and Thomas, 1982), which may be one of the major protolith of U-rich pegmatoids deriving from partial melting of the Wollaston metasediments (Mercadier et al., 2013). For example at Duddrige Lake, U-Cu mineralization, with 176 t U at 900 ppm, occurs within a metarkose with dark gray carbonaceous laminations and mottled areas (Delaney, 1993). The carbonaceous metarkose forms irregular lenses within a hematitic metarkose, which may be cut by pegmatoidic pods. Lewry and Sibbald (1979) already suggested strong similarities between the Duddridge Lake mineralization and uranium deposits from the Colorado Plateau area. Due to the

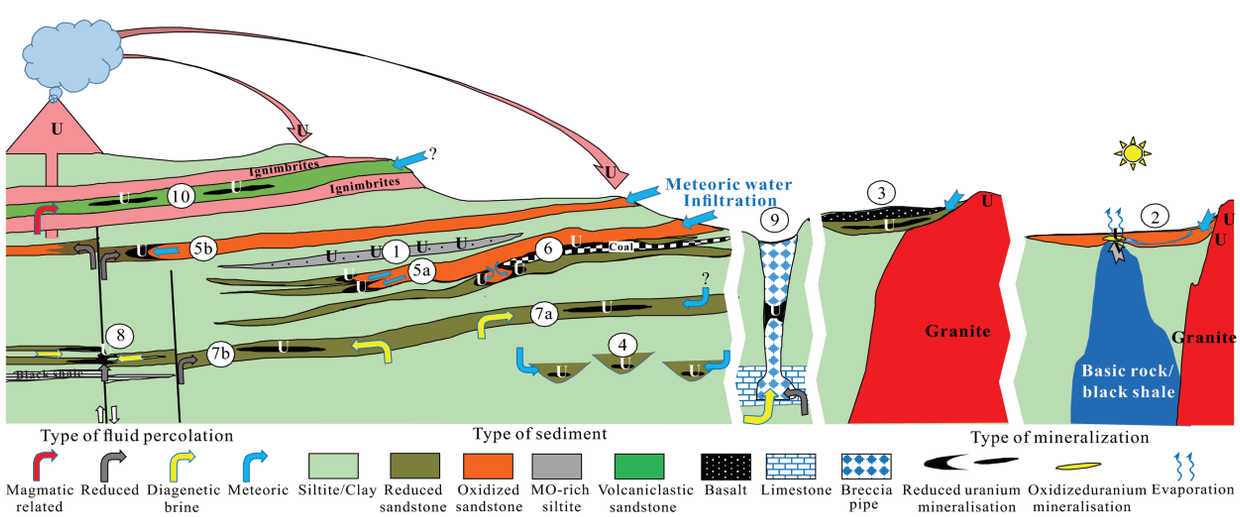

Figure 1. Schematic section illustrating the different types of sandstone related uranium deposits and the types of fluids involved in their genesis (I). (1) Synsedimentary uranium deposit; (2) evapotranspiration related uranium deposit; (3) sealed paleovalley; (4) valley confined amalgamated sandy meander-belts (VC-ASMB); (5a) roll front with intrinsic reductant; (5b) roll front with extrinsic reductant; (6) interstratified sandstone-lignite-coal uranium deposit; (7a) tabular deposit with intrinsic reductant; (7b) tabular deposit with extrinsic reductant; (8) tectono-lithologic deposit; (9) diagenetic-hydrothermal karst; (10) sedimentary-volcanic deposits.

absence of continental plant in Proterozoic sandstone, the carbon matter present within these metarkoses, which probably represent the reductant for the initial uranium deposition in these rocks, may derive from oil migration from black shale layers abundant within the Wollaston belt metasedimentary succession.

More recent and lower grade metamorphosed uranium mineralization in sandstone is known in the Permian formations of the Eastern Alpine Range in Switzerland, France and Austria. The sediments of Permian age are known to be the host of epigenetic, non-metamorphosed or metamorphosed, uranium mineralization all over Europe from Romania, Bulgaria to Italy and France (Dahlkamp, 2016). The Forstau uranium deposit located in the Austrian Alps described as a synmetamorphic deposit by Dahlkamp (2016 and references therein), is in fact a metamorphosed sandstone-hosted deposit. It is stratabound within a narrow belt of Permian formations mineralized discontinuously along a trend of about 10 km. The depositional environment varies from continental to near-shore environment from Forstau to Obertauern (Dahlkamp, 2016). Uranium resources of the Forstau deposit are estimated at 1 000–2 000 t U. The average grade is of 700 ppm–800 ppm U, but the uranium content varies significantly from place to place, from 0.005% to 2% U. The mineralized Permian horizons belong to thick pile of Triassic to Permian overthrust sheets. Most uranium mineralization in the Eastern Alps are hosted in Lower Permian sericitic quartzite and schists considered to be of continental origin and which have suffered low-grade metamorphism (400–450 °C) (Petraschek et al., 1977). The individual ore bodies are lenticular, with dimensions of 5–20 m along strike and down-dip, and with a thickness up to 2 m. They are tabular, parallel to the schistosity, but display an angle of about 20° to the general stratification, although no discordance between ore lenses and host strata has been observed. Uraninite and pitchblende are associated with framboidal pyrite and base metal sulphides and locally with black organic matter (Hellerschmidt-Alber, 2008). All these characteristics are typical of the epigenetic uranium mineralization from the Permian Basins all over Europe. It is remarkable that despite the metamorphic imprint, the texture of the framboidal pyrite has been preserved. More globally the metamorphism has not remobilized significantly the initial epigenetic uranium mineralization in the sandstone, probably because of the reducing conditions imposed by the presence of organic matter in the sediments, only local reconcentrations are observed in shear zones and in hinges of folds.

Another interesting example to discuss is the Eureka deposit in Catalonia, Spain recently reinterpreted as a metamorphite deposit (Castillo-Oliver et al., 2020). The Eureka V-Cu-U occurrences are located in the central Pyrenees, to the NW of the Pallars Jussà region in Catalonia. The Paleozoic basement was metamorphosed during the Hercynian orogeny. It was covered by Upper Carboniferous to Late Permian redbed unit with coal seams and calk-alkaline lavas and volcanoclastic interbeds, and Triassic to Cretaceous sediments. During the Alpine

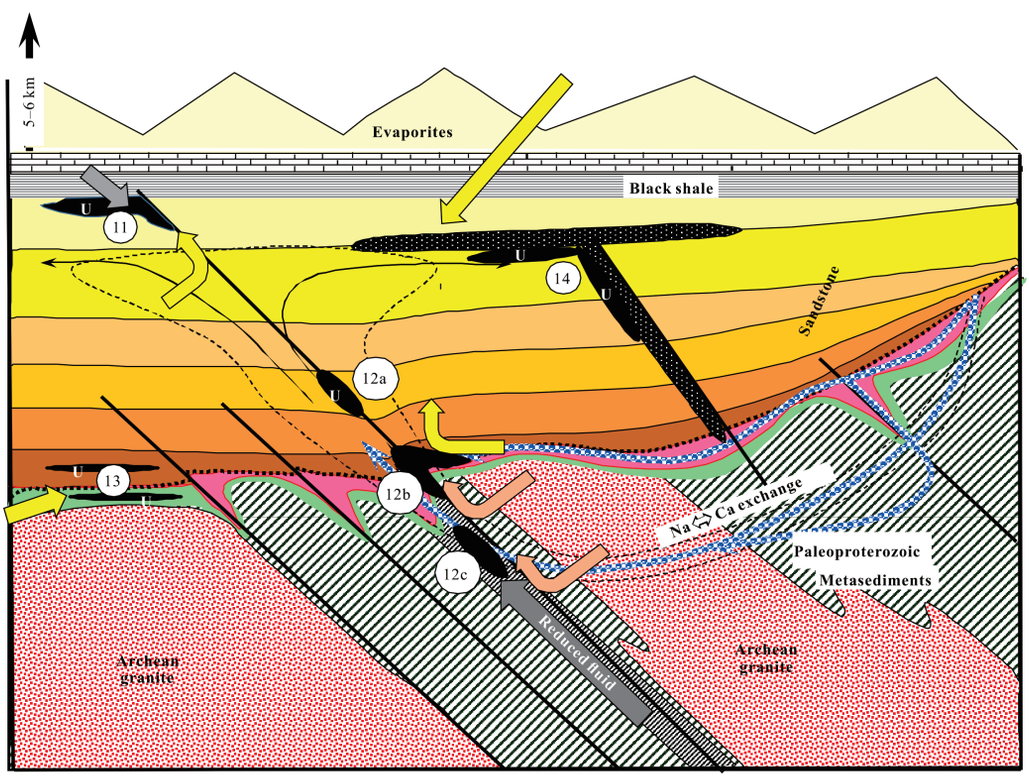

Figure 2. Schematic section illustrating the different types of sandstone related uranium deposits in oxidized Proterozoic sandstone basins, and the types of fluids involved in their genesis (II): (11) interformational redox control; (12a) basement/basin redox control, perched mineralization; (12b) basement/basin redox control, unconformity hosted uranium mineralization; (12c) basement/basin redox control, basement hosted mineralization; (13) basin/basement redox control; (14) mafic intrusion redox control. The blue arrows indicate the percolation of the diagenetic fluids into the basement to produce the Ca-U-rich brine from the Na-brine. Same symbols as in Fig. 1, except the orange arrows which indicate the Ca-U-riche brine.

orogeny in the Paleogene, deformation of the sedimentary/volcanic cover evolved to a pile of thrusts. The Triassic rocks have been submitted to very low-grade metamorphism, in the prehnite-pumpellyite facies. The Eureka V-Cu-U deposit is hosted in an Early Triassic (Buntsandstein) red-bed clastic series. The Early Trias consists in alluvial-fan polymictic conglomerates, followed by braided-river sandstone and mudstone with coal seam interbeds. The ore bodies are found in a 5 m thick greyish-green siliciclastic sedimentary unit, which overlay 50 m of reddish mudstones, interbedded with fine-grained sandstones. The greenish sediments are enriched in organic matter, present as detrital land plants and bituminous impregnations. The uranium mineralization is stratabound and occurs in up to 2 m thick lenses rich in organic matter. U-minerals are fine-grained and occur in the cement of the coarse sandstone units or follow the schistosity in the shale layers. The mineralization consists in a complex metallic element association: Cu-U-V-Ni-Co-As association. The cement comprises carbonates, quartz, roscoelite, V-rich muscovite, Ti-V oxides (schreyerite), xenotime, monazite, apatite, and a series of arsenides, sulphides, selenides, and U-oxides. Small veinlets, up to 1 cm wide, occur between the boudins developed in the competent sandstone layers. They are filled with drusy ankerite, barite, dolomite, and disseminated Cu-sulphides, but they are devoid of U-oxides.

Castillo-Oliver et al. (2020) suggest that the Eureka deposit corresponds to low-temperature metamorphite U deposit, hosted in sandstone. However, most of the features of this deposit correspond to an epigenetic tabular sandstone deposit: mineralization hosted in a reduced Triassic sandstone alternating with oxidized strata which represent one of common environments of U deposits in Europe (Dahlkamp, 2016), presence of disseminated detrital land plants, V-rich clay/mica minerals, a typical Cu-U-V-Ni-Co-As association, and the stratabound nature of the U mineralization. In addition no uranium is remobilized in the veinlets developed during the metamorphism, in coherence with the fact that uranium is not mobile during the metamorphism because of the reducing conditions imposed by the presence of synsedimentary organic matter.

7 CONCLUSIONS

Sandstone-related deposits are not only the most common type of uranium deposit on earth, but they are also probably the most diverse ones in terms of morphology, tonnages and grades of the ore bodies and of the conditions of their genesis. The present article proposes a new view on these deposits and on their classification, based on morphologic and genetic markers, and considering the main processes at the origin of the uranium accumulation (Table 1).

Many sandstone related deposits present transitional characteristics between the different deposit types defined above that are representing in fact endmembers: from purely meteoric fluid-driven to purely metamorphic fluid-driven deposit, through diagenetic fluid-driven, from wholly intrinsic reductant control to wholly extrinsic reductant control, from tabular to roll front shape, from entirely sedimentological-controlled deposits to entirely tectonic-controlled deposits, from purely syngenetic to purely epigenetic uranium concentration, from a fully intra-basin to fully basement setting, through deposits straddling the unconformity, from monometallic to polymetallic associations, with low to moderate temperatures of genesis, with very low to highly saline fluids, from non- to highly-

Table 1 Comparative characteristics of the various types of sandstone related uranium deposits

Type	Reductants	Temperature (°C)	Salinity wt.% eq. NaCl	Type example
Synsedimentary	Vascular land plants	Ambient	Very low	Nehuting, China
Meteoric fluid infiltration				
- Evapotranspiration	None	20–50	Very low	Yeleerie, Australia
- Sealed paleovalleys	Vascular land plants	10–20	Very low	Vitim, Russia
- VC-ASMB	Vascular land plants, bacterial sulfate red	20–40	Very low	Beverley, Australia
- Roll fronts	Vascular land plants, fluid from oil/gas basin, bacterial sulfate red	20–40	Very low	Wyoming, USA
- Interstratified sandstone-lignite-coal deposits	Vascular land plants, Lignite-coal	20–40	Very low	Koldzhatsk, Russia
Diagenetic hydrothermal				
- Intraformational redox control				
► Tabular	Vascular land plants, fluid from oil/gas res.	70–110	0–14	Uravan Belt, USA
► Tectonolithologic	Vascular land plants, fluid from oil/gas res.	130–250	3–14	Lodève, France
► Diagenetic-hydrothermal karsts	Fluid from oil/gas res.	80–170	4–17	Colorado Plateau USA
- Interformational redox control	Fluid from oil/gas res.	200	29–30	Oklo, Gabon
- Basement/basin redox control	Basement deriv. fluid, graphite/Fe-minerals	120–200	25–35	Athabasca, Canada
- Basin/basement redox control	Fluid from oil/gas res.	82–230	2–23	Koppunuru, India
- Mafic intrusion redox control	Fe minerals	99–380	Brines	Westmoreland, Austral.
Sedimentary-volcanic	?	?	?	Sierra Pintada, Argent.
Synmetamorphic	-	300–450	?	Camie River, Canada
Metamorphosed		400–750	-	Forstau, Austria

metamorphosed deposits. Sandstone deposit may occur from small intermontaneous basins to wide foreland, to marginal-marine sedimentary basins, from valley confined to laterally extensive amalgamated sandy meander-belt. Most sandstone-type uranium deposits have well-defined orebody boundaries, but some grade out progressively into less mineralized zones. Tabular uranium deposits seem to float within a sandstone layer without any visible relation to siltstone interbeds and overlying or underlying mudstones, whereas roll-front deposits are developed all over a sandstone layer between two bounding mudstones and their shape is also strongly controlled by the presence of mudstone interbeds.

Sandstone-related deposits are not limited to post-Silurian sedimentary basins, because mobile reductants (fluids or gases) necessary for the reduction of uranyl ions may be introduced into continental sandstone from other underlying geologic formations in which organic matter of marine origin is present.

ACKNOWLEDGMENTS

The authors are particularly grateful to the uranium exploration companies (especially ORANO and CAMECO) for the discussions, financial support and providing access to their properties. Patrice Bruneton is warmly thanked for a thorought revision of the manuscript. This paper is a contribution to the IGCP project 675 “Comparative analysis of mineralization of Sandstone-type U deposits”. The final publication is available at Springer via https://doi.org/10.1007/s12583-021-1532-x.

REFERENCES CITED

Adams, S. S., Smith, R. B., 1981. Geology and Recognition Criteria for Sandstone Uranium Deposits in Mixed Fluvial-Shallow Marine Sedimentary Sequences, South Texas. Final Report. Office of Scientific and Technical Information (OSTI). https://doi. org/10.2172/6554832

Ahamdach, N., Pagel, M., Mathis, V., 1993. Melt Inclusions in Apatite Crystals from Permian Cinerites in the Lodève Uraniferous Basin, France. *Comptes Rendus de le Academie des Sciences Serie Ii*, 316(7): 929–936

Ahmad, M., Wygralak, A. S., 1989. Calvert Hills, Northern Territory 1 : 250 000 Metallogenic Map Series, Sheet SE53-8. Northern Territory Geological Survey, Map and Explanatory Notes, Government Printer of the Northern Territory. 71

Alexandre, P., Kyser, K., Layton-Matthews, D., et al., 2015. Formation of the Enigmatic Matoush Uranium Deposit in the Paleoprotozoic Otish Basin, Quebec, Canada. *Mineralium Deposita*, 50(7): 825–845. https://doi.org/10.1007/s00126-014-0569-5

Alexandre, P., Kyser, K., Thomas, D., et al., 2009. Geochronology of Unconformity-Related Uranium Deposits in the Athabasca Basin, Saskatchewan, Canada and Their Integration in the Evolution of the Basin. *Mineralium Deposita*, 44(1): 41 – 59. https://doi. org/10.1007/s00126-007-0153-3

Annesley, I. R., Madore, C., Hajnal, Z., 2003. Wollaston-Mudjatik Transition Zone: Its Characteristics and Influence on the Genesis of Unconformity-Type Uranium Deposits. In: Cuney, M., ed., Uranium Geochemistry 2003, Conference Proceedings, Nancy. 55–58

Barton, I. F., Barton, M. D., Thorson, J. P., 2018. Characteristics of Cu and U-V Deposits in the Paradox Basin (Colorado Plateau) and Associated Alteration. *Society of Economic Geologists*, *Guidebook Series*, 59: 73–102

Beaufort, D., Rigault, C., Billon, S., et al., 2015. Chlorite and Chloritization Processes through Mixed-Layer Mineral Series in Low-Temperature Geological Systems—A Review. *Clay Minerals*, 50(4): 497 – 523. https://doi.org/10.1180/claymin.2015.050.4.06

Beyer, S. R., Kyser, K., Hiatt, E. E., et al., 2012. Basin Evolution and Unconformity-Related Uranium Mineralization: The Camie River U Prospect, Paleoproterozoic Otish Basin, Quebec. *Economic Geology*, 107(3): 401–425. https://doi.org/10.2113/econgeo.107.3.401

Boiron, M. C., Cathelineau, M., Richard, A., 2010. Fluid Flows and Metal Deposition near Basement/Cover Unconformity: Lessons and Analogies from Pb-Zn-F-Ba Systems for the Understanding of Proterozoic U Deposits. Frontiers in Geofluids. Wiley-Blackwell, Oxford. 270–292. https://doi.org/10.1002/9781444394900.ch19

Bonnetti, C., Cuney, M., Malartre, F., et al., 2015a. The Nuheting Deposit, Erlian Basin, NE China: Synsedimentary to Diagenetic Uranium Mineralization. *Ore Geology Reviews*, 69: 118 – 139. https://doi. org/10.1016/j.oregeorev.2015.02.010

Bonnetti, C., Cuney, M., Michels, R., et al., 2015b. The Multiple Roles of Sulfate-Reducing Bacteria and Fe-Ti Oxides in the Genesis of the Bayinwula Roll Front-Type Uranium Deposit, Erlian Basin, NE China. *Economic Geology*, 110(4): 1059–1081. https://doi. org/10.2113/econgeo.110.4.1059

Bonnetti, C., Liu, X. D., Yan, Z. B., et al., 2017. Coupled Uranium Mineralisation and Bacterial Sulphate Reduction for the Genesis of the Baxingtu Sandstone-Hosted U Deposit, SW Songliao Basin, NE China. *Ore Geology Reviews*, 82: 108 – 129. https://doi. org/10.1016/j.oregeorev.2016.11.013

Bonnetti, C., Zhou, L. L., Riegler, T., et al., 2020. Large S Isotope and Trace Element Fractionations in Pyrite of Uranium Roll Front Systems Result from Internally-Driven Biogeochemical Cycle. *Geochimica et Cosmochimica Acta*, 282: 113–132. https://doi.org/10.1016/j.gca.20 20.05.019

Bowell, R. J., Barnes, A., Grogan, J., et al., 2009. Geochemical Controls on Uranium Precipitation in in Calcrete Palaeochannel Deposits of Namibia, Proceedings of the 24th IAGS, Fredericton, New Brunswick. 413–418

Bray, C. J., Spooner, T. C., Longstaffe, F. J., 1988. unconformity-Related Uranium Mineralization, Mcclean Deposits, North Saskatchewan, Canada: Hydrogen and Oxygen Isotope Geochemistry. *The Canadian Mineralogist*, 26: 249–268

Brookins, D. G., 1980. Geochronologic Studies in the Grants Mineral Belt: New Mexico Bur. *Mines Mineral Resources*, *Memoires*, 38: 52–58

Caldeira, C. L., Ciminelli, V. S. T., Osseo-Asare, K., 2010. The Role of Carbonate Ions in Pyrite Oxidation in Aqueous Systems. *Geochimica et Cosmochimica Acta*, 74(6): 1777 – 1789. https://doi. org/10.1016/j.gca.2009.12.014

Cameron, E., Mazzucchelli, R. H., Robbins, T. W., 1980. Yeelirrie Calcrete Uranium Deposit, Murchison Region, Western Australia. *Journal of Geochemica Exploration*, 12(2–3): 350–353

Carlisle, D., 1984. Surficial Uranium Occurrences in Relation to Climate and Physical Setting. Surficial Uranium Deposits. IAEA-Tecdoc-322. Vienna. 25–35

Castillo-Oliver, M., Melgarejo, J. C., Torró, L., et al., 2020. Sandstone-Hosted Uranium Deposits as a Possible Source for Critical Elements: The Eureka Mine Case, Castell-Estaó, Catalonia. *Minerals*, 10(1): 34. https://doi.org/10.3390/min10010034

Cazoulat, M., 1985. Geological Environment of the Uranium Deposits in the Carboniferous and Jurassic Sandstones of the Western Margin of

the Aïr Mountains in the Republic of Niger. In: Geological Environment of Sandstone Type Uranium Deposits. I.A.E.A., Vienna, TECDOC, 328: 247–263

Cheng, Y. H., Wang, S. Y., Zhang, T. F., et al., 2020. Regional Sandstone-Type Uranium Mineralization Rooted in Oligo-Miocene Tectonic Inversion in the Songliao Basin, NE China. *Gondwana Research*, 88: 88–105. https://doi.org/10.1016/j.gr.2020.08.002

Chernonozhkin, S. M., Mercadier, J., Reisberg, L., et al., 2020. Evaluation of Rammelsbergite ($NiAs_2$) as a Novel Mineral for ^{187}Re-^{187}Os Dating and Implications for Unconformity-Related U Deposits. *Geochimica et Cosmochimica Acta*, 280: 85 – 101. https://doi.org/10.1016/j.gca.2020.04.011

Chi, G. X., Xue, C. J., 2014. Hydrodynamic Regime as a Major Control on Localization of Uranium Mineralization in Sedimentary Basins. *Science China Earth Sciences*, 57(12): 2928 – 2933. https://doi. org/10.1007/s11430-014-4976-3

Chi, G., Chu, H., Petts, D., et al., 2019. Uranium-Rich Diagenetic Fluids Provide the Key to Unconformity-Related Uranium Mineralization in the Athabasca Basin. *Scientific Reports*, 9(1): 5530. https://doi. org/10.1038/s41598-019-42032-0

Chi, G., Li, Z., Chu, H., et al., 2018. A Shallow-Burial Mineralization Model for the Unconformity-Related Uranium Deposits in the Athabasca Basin. *Economic Geology*, 113(5): 1209 – 1217. https://doi.org/10.5382/econgeo.2018.4588

Chown, E. H., 1979. Structure and Metamorphism of the Otish Mountain Area of the Grenvillian Foreland Zone, Québec: Summary. *Geological Society of America Bulletin*, 90(1): 13 – 15. https://doi. org/10.1130/0016-7606(1979)9013: samoto>2.0.co;2

Chudasama, B., Porwal, A., González- Álvarez, I., et al., 2018. Calcrete-Hosted Surficial Uranium Systems in Western Australia: Prospectivity Modeling and Quantitative Estimates of Resources. Part 1 – Origin of Calcrete Uranium Deposits in Surficial Environments: A Review. *Ore Geology Reviews*, 102: 906–936. https://doi. org/10.1016/j. oregeorev.2018.04.024

Comte, D., Blachère, H., Varlet, M., 1985. Geological Environment of the Uranium Deposits in the Permian of Lodève Basin, France. In "Geological Environments of Sandstone-Type Uranium Deposits", IAEA TECDOC 328, Vienna. 248

Cui, T., Yang, J., Samson, I. M., 2012. Tectonic Deformation and Fluid Flow: Implications for the Formation of Unconformity-Related Uranium Deposits. *Economic Geology*, 107(1): 147 – 163. https://doi.org/10.2113/econgeo.107.1.147

Cuney, M., 2010. Evolution of Uranium Fractionation Processes through Time: Driving the Secular Variation of Uranium Deposit Types. *Economic Geology*, 105(3): 553–569. https://doi.org/10.2113/gseconge o.105.3.553

Cuney, M., 2014. Felsic Magmatism and Uranium Deposits. *Bulletin de la Société Géologique de France*, 185(2): 75–92. https://doi.org/10.2113/gssgfbull.185.2.75

Cuney, M., 2011. Uranium and Thorium: The Extreme Diversity of the Resources of the World's Energy Minerals. In: Sinding-Larsen, R., Wellmer, F. W., eds., Non-Renewable Resource Issues: Geoscientific and Societal Challenges, International Year of Planet Earth, Springer. 91–129

Cuney, M., Kyser, K., 2015. Geology and Geochemistry of Uranium and Thorium Deposits. *Mineralogical Association of Canada*, 46: 362

Cuney, M., Mathieu, R., 2000. Extreme Light Rare Earth Element Mobilization by Diagenetic Fluids in the Geological Environment of the Oklo Natural Reactor Zones, Franceville Basin, Gabon. *Geology*, 28(8): 743 – 746. https://doi. org/10.1130/0091-7613(2000)28743: elree m>2.0.co;2

Dahlkamp, F. J., 2016. Uranium Deposits of the World. Springer, Berlin. 485–496. https://doi.org/10.1007/978-3-540-78554-5_10

Dahlkamp, F. J., 1993. Uranium Ore Deposits, Springer-Verlag, Berlin. 460

Dahlkamp, F. J., 2009. Uranium Deposits of the World: Asia. Springer-Verlag, Berlin. 494

Dargent, M., Truche, L., Dubessy, J., et al., 2015. Reduction Kinetics of Aqueous U(VI) in Acidic Chloride Brines to Uraninite by Methane, Hydrogen or C-Graphite under Hydrothermal Conditions: Implications for the Genesis of Unconformity-Related Uranium Ore Deposits. *Geochimica et Cosmochimica Acta*, 167: 11 – 26. https://doi. org/10.1016/j.gca.2015.06.027

Dayboll, R., Rainbird, R., Hahn, K., 2010. Characterization of Mineralization and Deposit Style of the Mountain Lake Uranium Deposit, Hornby Bay Basin, Nunavut. AAPG Search and Discovery Article, GeoConvention 2010, Calgary

De Voto, R. H., 1978. Uranium Geology and Exploration: Lecture Notes and References. Colorado School of Mines, Golden. 396

Delaney, G. D., 1993. A Re-Examination of the Context of U-Cu, Cu, and U Mineralization, Duddridge Lake, Wollaston Domain, In: Summary of Investigations 1993, Saskatchewan Geological Survey, Sask

Derome, D., Cathelineau, M., Cuney, M., et al., 2005. Mixing of Sodic and Calcic Brines and Uranium Deposition at McArthur River, Saskatchewan, Canada: A Raman and Laser-Induced Breakdown Spectroscopic Study of Fluid Inclusions. *Economic Geology*, 100(8): 1529–1545. https://doi.org/10.2113/gsecongeo.100.8.1529

Derome, D., Cuney, M., Cathelineau, M., et al., 2003. A Detailed Fluid Inclusion Study in Silicified Breccias from the Kombolgie Sandstones (Northern Territory, Australia): Inferences for the Genesis of Middle-Proterozoic Unconformity-Type Uranium Deposits. *Journal of Geochemical Exploration*, 80(2/3): 259 – 275. https://doi. org/10.1016/S0375-6742(03)00194-8

Dickinson, K. A., Duval, J. S., 1977. South-Texas Uranium: Geologic Controls, Exploration Techniques, and Potential, In: Campbell, M. D., ed., Geology of Alternate Energy Resources. Houston Geological Society, Houston. 45–66

Dickinson, W. R., Gehrels, G. E., 2008. U-Pb Ages of Detrital Zircons in Relation to Paleogeography: Triassic Paleodrainage Networks and Sediment Dispersal across Southwest Laurentia. *Journal of Sedimentary Research*, 78(12): 745 – 764. https://doi. org/10.2110/jsr.2008.088

Douglas, G. B., Butt, C. R. M., Gray, D. J., 2011. Geology, Geochemistry and Mineralogy of the Lignite-Hosted Ambassador Palaeochannel Uranium and Multi-Element Deposit, Gunbarrel Basin, Western Australia. *Mineralium Deposita*, 46(7): 761 – 787. https://doi. org/10.1007/s00126-011-0349-4

Eargle, D. H., Weeks, A. D., 1961. Possible Relation between Hydrogen Sulfide-Bearing Hydrocarbons in Fault-Line Oil Fields and Uranium Deposits in the Southeast Texas Coastal Plain. US Geol. Survey. Profess. 424

Eglinger, A., André -Mayer, A. S., Vanderhaeghe, O., et al., 2013. Geochemical Signatures of Uranium Oxides in the Lufilian Belt: From Unconformity-Related to Syn-Metamorphic Uranium Deposits during the Pan-African Orogenic Cycle. *Ore Geology Reviews*, 54: 197–213. https://doi.org/10.1016/j.oregeorev.2013.04.003

Fayek, M., Kyser, T. K., 1997. Characterization of Multiple Fluid-Flow

Events and Rare Earth-Element Mobility Associated with Formation of Unconformity-Type Uranium Deposits in the Athabasca Basin, Saskatchewan, *Canadian Mineralogist*, 35(3): 627–658

Finch, W. I., 1996. Uranium Provinces of North America—Their Definition, Distribution, and Models. United States Geological Survey Bulletin, Washington, D. C. https://doi.org/10.3133/b2141

Finch, W. I., Davis, J. F., 1985. Sandstone-Type Uranium Deposits—An Introduction. In: Geological Environments of Sandstone-Type Uranium Deposits, IAEA TECDOC-328, International Atomic Energy Agency, Vienna. 11–21

Fischer, R. P., 1942. Vanadium Deposits of Colorado and Utah, a Preliminary Report. US Geological Survey, Washington, D. C. https://doi.org/10.3133/b936p

Forbes, P., 1988. Rôles des Structures Sédimentaires et Tectoniques, du Volcanisme Alcalin Régional et des Fluides Diagénétiques-Hydrothermaux Pour la Formation des Minéralisations à U-Zr-Zn-V-MO d'Akouta (Niger). *Géol. Géochim. Mém*., 17: 387

Forbes, P., Pacquet, A., Chantret, F., et al., 1984. Marqueurs du Volca NISME dans le Gisement Duranium d'Akouta (République du Niger). *Compte Rendus à l'Académie des Sciences*, 298(II-15): 647–650

Gancarz, A. J., 1977. U-Pb Age (2.05×10^9 Years) of the Oklo Uranium Deposit. In: IAEA Symposium on Natural Fission Reactors, Paris, Dec. 19–21, 1977

Garven, G., 1999. Proterozoic Basins, Fluids and Giant Ore Deposits of Northern Australia. *Sciences Geologiques*, 99: 71–74

Gatzweiler, R., 1987. Uranium Mineralization in the Proterozoic Otish Basin, Central Quebec, Canada, In: Friedrich, G., Gatzweiler, R., Vogt, J., eds., Uranium Mineralization—New Aspects on Geology, Mineralogy, Geochemistry and Exploration Methods. Gebrüder Borntraeger, Berlin-Stuttgart

Gauthier-Lafaye, F., 1986. Les Gisements d'Uranium du Gabon et Les Réacteurs d'Oklo. Modèle Métallogénique de Gîtes à Fortes Teneurs du Protérozoïque Iinférieur, Sciences Géologiques, *Bulletins et Mémoires*, 78: 206

Gauthier-Lafaye, F., Weber, F., 1989. The Francevillian (Lower Proterozoic) Uranium Ore Deposits of Gabon. *Economic Geology*, 84(8): 2267–2285. https://doi.org/10.2113/gsecongeo.84.8.2267

Genest, S., 1989. Histoire Géologique du Bassin d'Otish, Protérozoïque Inférieur (Québec): [Dissertation]. Université de Montréal, Montréal. 329

Gerbeaud, O., 2006. Evolution Structurale du Bassin de Tim Mersoï le Rôle des Déformations de la Couverture Sédimentaire sur la Mise en Place des Gisements Uranifère du Secteur d Arlit (Niger): [Dissertation]. Paris-Sud University, Orsay. 276

Gigon, J., 2019. Dynamics of the McArthur Basin Diagenetic/Hydrothermal System (Australia): Timing and Nature of Fluid Flow and Constraints on the Distribution of Mineral Resources (U, Cu, Pb-Zn): [Dissertation], Univ. Lorraine, Nancy. 404

Gigon, J., Mercadier, J., Annesley, I. R., et al., 2021. Uranium Mobility and Deposition over 1.3 Ga in the Westmoreland Area (McArthur Basin, Australia). *Mineralium Deposita*, 56(7): 1321–1344. https://doi.org/10.1007/s00126-020-01031-2

Giles, D., Nutman, A. P., 2002. SHRIMP U-Pb Monazite Dating of 1 600–1 580 Ma Amphibolite Facies Metamorphism in the Southeastern Mt Isa Block, Australia. *Australian Journal of Earth Sciences*, 49(3): 455–465. https://doi.org/10.1046/j.1440-0952.2002.00931.x

Goldhaber, M. B., Reynolds, R. L., Rye, R. O., 1979. Formation and Resulfidization of a South Texas Roll-Type Uranium Deposit. U. S. Geological Survey Open-File Report 79-1651: 41

Granger, H. C., Warren, C. G., 1979. The Importance of Dissolved Free Oxygen during Formation of Sandstone-Type Uranium Deposits. U.S. Geological Survey Open-File Report. 79-1603: 1–22

Hall, S. M., Mihalasky, M. J., Tureck, K., et al., 2017. Genetic and Grade and Tonnage Models for Sandstone-Hosted Roll-Type Uranium Deposits, Texas Coastal Plain, USA. *Ore Geology Reviews*, 80: 716–753

Hamilton, M. A., Buchan, K. L., 2016. A 2 169 Ma U-Pb Baddeleyite Age for the Otish Gabbro, Quebec: Implications for Correlation of Proterozoic Magmatic Events and Sedimentary Sequences in the Eastern Superior Province. *Canadian Journal of Earth Sciences*, 53(2): 119–128. https://doi.org/10.1139/cjes-2015-0131

Hanly, A., 2005. Evolution of Mesoproterozoic Basins and Their Economic Potential: [Dissertation]. Queen's University, Kingston. 276

Hartley, A. J., Owen, A., Weissmann, G. S., et al., 2018. Modern and Ancient Amalgamated Sandy Meander-Belt Deposits: Recognition and Controls on Development. *Int. Assoc. Sedimentology Special Publication*, 48: 349–384

Hartley, A. J., Weissmann, G. S., Nichols, G. J., et al., 2010. Large Distributive Fluvial Systems: Characteristics, Distribution, and Controls on Development. *Journal of Sedimentary Research*, 80(2): 167–183. https://doi.org/10.2110/jsr.2010.016

Hecht, L., Cuney, M., 2000. Hydrothermal Alteration of Monazite in the Precambrian Crystalline Basement of the Athabasca Basin (Saskatchewan, Canada): Implications for the Formation of Unconformity-Related Uranium Deposits. *Mineralium Deposita*, 35 (8): 791–795. https://doi.org/10.1007/s001260050280

Hellerschmidt-Alber, J., 2008. Geologie des Gebietes Südlich von Forstau im Ennstal auf ÖK 126 Radstadt (Bundesland Salzburg). *Jahrbuch der Geologischen Bundesanstalt*, 148(2): 159–173

Hoeve, J., Quirt, D., 1987. A Stationary Redox Front as a Critical Factor in the Formation of High-Grade, Unconformity-Type Uranium Ores in the Athabasca Basin, Saskatchewan, Canada. *Bulletin de Minéralogie*, 110(2): 157–171. https://doi.org/10.3406/bulmi.1987.7977

Höhndorf, A., Bianconi, F., Pechmann, E. V., 1987. Geochronology and Metallogeny of Vein-Type Uranium Occurrences in the Otish Basin Area, Quebec, Canada, in Metallogenesis of Uranium Deposits. Proceedings of a Technical Committee: IAEA, Vienna. 233–260

Hynes, A., Rivers, T., 2010. Protracted Continental Collision-Evidence from the Grenville Orogen. *Canadian Journal of Earth Sciences*, 47 (5): 591–620. https://doi.org/10.1139/e10-003

IAEA, 2009. World Distribution of Uranium Deposits (UDEPO) with Uranium Deposit Classification. IAEA TECDOC 1629, Vienna. 128

IAEA, 2016. World Distribution of Uranium Deposits (UDEPO). IAEA TECDOC 1843, Vienna. 262

IAEA, 2018a. Geological Classification of Uranium Deposits and Description of Selected Examples. IAEA TECDOC 1842, Vienna. 248

IAEA, 2018b. Unconformity Related Deposits. IAEA TECDOC 1857, Vienna. 298

Jefferson, C. W., Thomas, D. J., Gandhi, S. S., et al., 2007. Unconformity-Associated Uranium Deposits of the Athabasca Basin, Saskatchewan and Alberta. In: Goodfellow, W. D., ed., Mineral Deposits of Canada: A Synthesis of Major Deposit Types, District Metallogeny, The Evolution of Geological Provinces, and Exploration Methods. *Geological Association of Canada*, 5: 273–305

Jia, J. M., Rong, H., Jiao, Y. Q., et al., 2020. Mineralogy and Geochemistry of Carbonate Cement in Sandstone and Implications for Mineralization

of the Qianjiadian Sandstone-Hosted Uranium Deposit, Southern Songliao Basin, China. *Ore Geology Reviews*, 123: 103590. https://doi.org/10.1016/j.oregeorev.2020.103590

Jin, R. S., Teng, X. M., Li, X. G., et al., 2020. Genesis of Sandstone-Type Uranium Deposits along the Northern Margin of the Ordos Basin, China. *Geoscience Frontiers*, 11(1): 215–227. https://doi.org/10.1016/j.gsf.2019.07.005

Kish, L., Cuney, M., 1981. Uraninite-Albite Veins from the Mistamisk Valley of the Labrador Trough, Quebec. *Mineralogical Magazine*, 44 (336): 471–483. https://doi.org/10.1180/minmag.1981.044.336.13

Kislyakov, Ya. M., Shchetochkin, V. N., 2000. Hydrogenic Ore Formation. Geoinformmark, Moscow. 608 (in Russian)

Kleiman, L. E., 1999. Mineralogía y Petrología del Volcanismo Permo-Triásico y Triásico del Bloque de San Rafael en el área de Sierra Pintada, Provincia de Mendoza, y su Relación con las Mineralizaciones de Uranio: [Dissertation], Facultad de Ciencias Exactas y Naturales, Universidad de Buenos Aires, Buenos Aires. 286 (in Spanish)

Klingmuller, L. M. L., 1989. The Green Mountain Uranium District, Central Wyoming: Type Locality of Solution Front Limb Deposits. *IAEA-Tecdoc*, 500: 173–190

Kochkin, B. T., Tarasov, N. N., Andreeva, O. V., et al., 2017. Polygenetic and Polychronic Uranium Mineralization at Deposits of the Khiagda Ore Field, Buryatia. *Geology of Ore Deposits*, 59(2): 141–155. https://doi.org/10.1134/S1075701517020015

Kyser, K., Cuney, M., 2015. Basin and Uranium Deposits. In: Cuney, M., Kyser, K., eds., The Geology and Geochemistry of Uranium and Thorium Deposits, *Mineralogical Association of Canada*, 46: 225–304

Lach, P., 2012. Signature Géochimique des Eléments des Terres Rares Dans les Oxydes D'uranium et Minéraux Associés Dans les Gisements D'uranium : Analyse par Ablation Laser Couplée à l'ICP-MS et étude Géochronologique: [Dissertation], Univ. Lorraine, Nancy. 296

Lancelot, J., Vella, V., 1989. Datation U-Pb Liasique de La Pechblende de Rabejac; Mise en Evidence D ' une Preconcentration Uranifere Permienne Dans le Bassin de Lodeve (Herault). *Bulletin de la Société Géologique de France*, V(2): 309 – 315. https://doi. org/10.2113/gssgfbull.v.2.309

Landais, P., 1986. Geochemical Analyses of the Organic Matter Associated with the Breccia Pipes in the Grand Canyon Area. *Geological Society of America Abstracts with Programs*, 18: 389

Landais, P., 1993. Bitumens in Uranium Deposits. In: Parnell, J., Kucha, H., Landais, P., eds., Bitumens in Ore Deposits. Springer-Verlag, Berlin, 213–238

Landais, P., Connan, J., 1986. Source Rock Potential and Oil Alteration in the Uraniferous Basin of Lodève (Hérault, France). Potentiel Pétrolier et Dégradation des Huiles Dans Le Bassin Uranifère de Lodève (Hérault, France). *Sciences Géologiques Bulletin*, 39(3): 293 – 314. https://doi.org/10.3406/sgeol.1986.1732

Le Carlier De Veslud, C., Cuney, M., Lorilleux, G., et al., 2009. 3D Modeling of Uranium-Bearing Solution-Collapse Breccias in Proterozoic Sandstones (Athabasca Basin, Canada) —Metallogenic Interpretations. *Computers & Geosciences*, 35(1): 92–107. https://doi.org/10.1016/j.cageo.2007.09.008

Lecomte, A., Michels, R., Cathelineau, M., et al., 2020. Uranium Deposits of Franceville Basin (Gabon): Role of Organic Matter and Oil Cracking on Uranium Mineralization. *Ore Geology Reviews*, 123: 103579. https://doi.org/10.1016/j.oregeorev.2020.103579

Lesbros-Piat-Desvial, M., Beaudoin, G., Mercadier, J., et al., 2017. Age and Origin of Uranium Mineralization in the Camie River Deposit (Otish Basin, Québec, Canada). *Ore Geology Reviews*, 91: 196–215. https://doi.org/10.1016/j.oregeorev.2017.10.006

Lewis, S. R., Trimble, D. E., 1959. Geology and Uranium Deposits of Monument Valley San Juan County, Utah. USGS Prof. Pap. 1087D, 121–131

Lewry, J. F., Sibbald, T. I. I., 1979. A review of pre-Athabasca Basement Geology in Northern Saskatchewan, In: Parslow, G. R., ed., Uranium Exploration Techniques. *Saskatchewan Geological Society Special Publication*, 4: 19–58

Lorilleux, G., Jébrak, M., Cuney, M., et al., 2002. Polyphase Hydrothermal Breccias Associated with Unconformity-Related Uranium Mineralization (Canada): From Fractal Analysis to Structural Significance. *Journal of Structural Geology*, 24(2): 323–338. https://doi.org/10.1016/S0191-8141(01)00068-2

Ludwig, K. R., Simmons, K. R., 1992. U-Pb Dating of Uranium Deposits in Collapse Breccia Pipes of the Grand Canyon Region. *Economic Geology*, 87(7): 1747–1765. https://doi.org/10.2113/gsecongeo.87.7.1747

Ludwig, K. R., Simmons, K. R., Webster, J. D., 1984. U-Pb Isotope Systematics and Apparent Ages of Uranium Ores, Ambrosia Lake and Smith Lake Districts, Grants Mineral Belt, New Mexico. *Economic Geology*, 79(2): 322–337. https://doi.org/10.2113/gsecongeo.79.2.322

Maksimova, M. F., Shmariovich, E. M., 1993. Bedded-Infiltrational Ore Formation. Nedra, Moscow. 160 (in Russian)

Mamadou, M. M., Cathelineau, M., Bourdelle, F., et al., 2016. Hot Fluid Flows around a Major Fault Identified by Paleothermometric Studies (Tim Mersoï Basin, Niger). *Journal of Sedimentary Research*, 86(8): 914–928. https://doi.org/10.2110/jsr.2016.62

Mamadou, M. M., 2016. Le Système Métallogénique des Gisements d' Uranium Associés à la Faille d-Arlit (Bassin de Tim Mersoï, Niger): Diagenèse, Circulations des Fluides et Mécanismes D'enrichissement en métaux (U, Cu, V): [Dissertation]. Univ. Lorraine, Nancy. 402

Martin, M. S., 1992. Genèse et Evolution Structural du Bassin Permien de Lodéve (Hérault-France). Cuadernos de Geologia Iberica, Editoria Complutense, Madrid. 16: 75–90

Mashkovtsev, G. A., Kochenov, A. V., Khaldey, A. E., 1995. On Hydrothermal Sedimentary Formation of Stratiform Uranium Deposits in Phanerozoic Depressions. Rare-Metal-Uranium Ore Formation within Sedimentary Rocks. Nauka, Moscow. 37–51 (in Russian)

Mathieu, R., Cuney, M., Cathelineau, M., 2000. Geochemistry of Palaeofluids Circulation in the Franceville Basin and around Oklo Natural Nuclear Reaction Zones (Gabon). *Journal of Geochemical Exploration*, 69/70: 245–249. https://doi. org/10.1016/s0375-6742(00)00054-6

Mathieu, R., Deschamps, Y., Selezneva, V., et al., 2015. Key Mineralogical Characteristics of the New South Tortkuduk Uranium Roll-Front Deposits, Kazakhstan. Conference: 13th SGA Biennal Meeting, August 2015, Nancy. 1835–1838

Mathis, V., Robert, J. P., Saint Martin, J., 1990. Géologie et Métallogénie des Gisements D ' uranium du Bassin Permien de Lodève (sud du Massif Central Français). *Chronique de la Recherche Minière*, 58 (499): 31–40

McLemore, V. T., 2010. The Grants Uranium District, New Mexico: Update on Source, Deposition, and Exploration. *The Mountain Geologist*, 48: 23–44

Meek, A., 2014. Sandstone Uranium Deposits of Nebraska and Colorado: A Comparative Study: [Dissertation]. Manitoba University, Manitoba. 141

Mendez Santizo, J., Gauthier-Lafaye, F., Liewig, N., et al., 1991. Existence d ' un Hydrothermalisme tardif Dans le Bassin de Lodève (Hérault). Arguments PaléOTHERMO Métriques et Géochronologiques. *Compte Rendus à L'Académie des Sciences*, 312: 739–745

Mercadier, J., Annesley, I. R., McKechnie, C. L., et al., 2013. Magmatic and Metamorphic Uraninite Mineralization in the Western Margin of the Trans-Hudson Orogen (Saskatchewan, Canada): A Uranium Source for Unconformity-Related Uranium Deposits? *Economic Geology*, 108(5): 1037–1065. https://doi.org/10.2113/econgeo.108.5.1037

Mercadier, J., Cuney, M., Lach, P., et al., 2011. Origin of Uranium Deposits Revealed by Their Rare Earth Element Signature. *Terra Nova*, 23(4): 264–269. https://doi.org/10.1111/j.1365-3121.2011.01008.x

Mernagh, T. P., Wygralak, A. S., 2011. A Fluid Inclusion Study of Uranium and Copper Mineral Systems in the Murphy Inlier, Northern Australia. *Russian Geology and Geophysics*, 52(11): 1421–1435. https://doi.org/10.1016/j.rgg.2011.10.011

Meunier, J. D., 1994. The Composition and Origin of Vanadium-Rich Clay Minerals in Colorado Plateau Jurassic Sandstones. *Clays and Clay Minerals*, 42(4): 391–401. https://doi.org/10.1346/CCMN.1994.0420403

Meunier, J. D., Landais, P., Monthioux, M., et al., 1987. Oxidation-Reduction Processes in the Genesis of the Uranium-Vanadium Tabular Deposits of the Cottonwood Wash Mining Area (Utah, USA): Evidence from Petrological Study and Organic Matter Analysis. *Bulletin de Minéralogie*, 110(2): 145 – 156. https://doi. org/10.3406/bulmi.1987.7976

Miller, D. S., Laurence Kulp, J., 1963. Isotopic Evidence on the Origin of the Colorado Plateau Uranium Ores. *Geological Society of America Bulletin*, 74(5): 609 – 630. https://doi. org/10.1130/0016-7606(1963)74[609: ieotoo]2.0.co;2

Min, M. Z., Luo, X. Z., Mao, S. L., et al., 2002. The Saqisan Mine—A Paleokarst Uranium Deposit, South China. *Ore Geology Reviews*, 19(1/2): 79–93. https://doi.org/10.1016/S0169-1368(00)00010-X

Mueller, A., Halbach, P., 1983. The Anderson Mine (Arizona), An Early Diagenetic Uranium Deposit in Miocene Lake Sediments. *Economic Geology*, 78(2): 275–292. https://doi.org/10.2113/gsecongeo.78.2.275

Nakashima, S., Disnar, J. R., Perruchot, A., et al., 1987. Fixation et Réduction de L ' uranium Par Les Matières Organiques Naturelles: Mécanismes et Aspects Cinétiques. *Bulletin de Minéralogie*, 110(2): 227–234. https://doi.org/10.3406/bulmi.1987.7982

Nash, J. T., Granger, H. C., Adams, S. S, 1981. Geology and Concepts of Genesis of Important Types of Uranium Deposits. *Society of Economic Geologists*, 75: 63–116. https://doi.org/10.5382/av75.04

Ndongo, A., Guiraud, M., Vennin, E., et al., 2016. Control of Fluid-Pressure on Early Deformation Structures in the Paleoproterozoic Extensional Franceville Basin (SE Gabon). *Precambrian Research*, 277: 1 – 25. https://doi.org/10.1016/j.precamres.2016.02.003

Northrop, H. R., Goldhaber, M. B., Landis, G. P., et al., 1990. Genesis of the Tabular-Type Vanadium-Uranium Deposits of the Henry Basin, Utah. *Economic Geology*, 85(2): 215 – 269. https://doi. org/10.2113/gsecongeo.85.2.215

Nuccio, V. F., Condon, S. M., 2000. Burial and Thermal History of the Paradox Basin, Utah and Colorado, and Petroleum Potential of the Middle Pennsylvanian Paradox Basin. US Geological Survey. Washington, D. C. https://doi.org/10.3133/b00o

Orth, K., 2010. Geology, Volcanology and Mineral Potential of the Cliffdale and Seigal Volcanics, Calvert Hills 1 : 250 000 Geological Map Sheet, SE 53-08, Northern Territory. Northern Territory Geological Survey, Record 2010-003

Pagel, M., Cavellec, S., Forbes, P., et al., 2005. Uranium Deposits in the Arlit Area (Niger). Mineral Deposit Research: Meeting the Global Challenge. Springer, Berlin. https://doi.org/10.1007/3-540-27946-6_79

Parslow, G. R., Thomas, D. J., 1982. Uranium Occurrences in the Cree Lake Zone, Saskatchewan, Canada. *Mineralogical Magazine*, 46(339): 163–171. https://doi.org/10.1180/minmag.1982.046.339.02

Partin, C. A., Bekker, A., Planavsky, N. J., et al., 2013. Large-Scale Fluctuations in Precambrian Atmospheric and Oceanic Oxygen Levels from the Record of U in Shales. *Earth and Planetary Science Letters*, 369/370: 284–293. https://doi.org/10.1016/j.epsl.2013.03.031

Pechenkin, I., 2014. Sandstone Uranium Deposits of Eurasia: From Genetic Concepts to Forecasting New Discoveries. URAM 2014. IAEA, Vienna. 68

Petrascheck, W. E., Erkan, E., Siegl, W., 1977. Types of Uranium Deposits in the Austrian Alps, Geology, Mining and Extractive Processing of Uranium (Proc. Int. Symp. London, 1977), Institution of Mining and Metallurgy, London. 71 – 75

Polito, P. A., Kyser, T. K., Rheinberger, G., et al., 2005. A Paragenetic and Isotopic Study of the Proterozoic Westmoreland Uranium Deposits, Southern McArthur Basin, Northern Territory, Australia. *Economic Geology*, 100(6): 1243 – 1260. https://doi.org/10.2113/gsecongeo.100.6.1243

Ramm, M., 1992. Porosity-Depth Trends in Reservoir Sandstones: Theoretical Models Related to Jurassic Sandstones Offshore Norway. *Marine and Petroleum Geology*, 9(5): 553 – 567. https://doi. org/10.1016/0264-8172(92)90066-N

Renac, C., Kyser, T. K., Durocher, K., et al., 2002. Comparison of Diagenetic Fluids in the Proterozoic Thelon and Athabasca Basins, Canada: Implications for Protracted Fluid Histories in Stable Intracratonic Basins. *Canadian Journal of Earth Sciences*, 39(1): 113–132. https://doi.org/10.1139/e01-077

Richard, A., Banks, D. A., Mercadier, J., et al., 2011. An Evaporated Seawater Origin for the Ore-Forming Brines in Unconformity-Related Uranium Deposits (Athabasca Basin, Canada): Cl/Br and δ^{37}Cl Analysis of Fluid Inclusions. *Geochimica et Cosmochimica Acta*, 75(10): 2792–2810. https://doi.org/10.1016/j.gca.2011.02.026

Richard, A., Rozsypal, C., Mercadier, J., et al., 2012. Giant Uranium Deposits Formed from Exceptionally Uranium-Rich Acidic Brines. *Nature Geoscience*, 5(2): 142–146. https://doi.org/10.1038/ngeo1338

Robbins, M., 2009. Sedimentology and Sedimentary Tectonics of the Salt Wash Member, Morrison Formation, Western Colorado: [Dissertation]. Boston College, Boston. 75

Rong, H., Jiao, Y. Q., Liu, X. F., et al., 2020. Effects of Basic Intrusions on REE Mobility of Sandstones and Their Geological Significance: A Case Study from the Qianjiadian Sandstone-Hosted Uranium Deposit in the Songliao Basin. *Applied Geochemistry*, 120: 104665. https://doi.org/10.1016/j.apgeochem.2020.104665

Rong, H., Jiao, Y. Q., Wu, L. Q., et al., 2019. Origin of the Carbonaceous Debris and Its Implication for Mineralization within the Qianjiadian Uranium Deposit, Southern Songliao Basin. *Ore Geology Reviews*, 107: 336–352. https://doi.org/10.1016/j.oregeorev.2019.02.036

Salze, D., Belcourt, O., Harouna, M., 2018. The First Stage in the Formation of the Uranium Deposit of Arlit, Niger: Role of a New Non-Continental Organic Matter. *Ore Geology Reviews*, 102: 604 – 617. https://doi.org/10.1016/j.oregeorev.2018.09.021

Sanford, R. F., 1992. A New Model for Tabular-Type Uranium Deposits. *Economic Geology*, 87(8): 2041–2055. https://doi. org/10.2113/gsecongeo.87.8.2041

Sanguinetti, H., Oumarou, J., Chantret, F., 1982. Localisation de Luranium dans les Figures de Sédimentation des Grès Hôtes du Gisement d'Akouta, République du Niger. *Compte Rendus à l'Académie des Sciences*, 264(II): 591–594

Sani, A., Konaté, M., Karimou, D. H., et al., 2020. Polyphasic Tectonic History of the N70° DASA Graben (Northern, Niger). *Global Journal of Earth and Environmental Science*, 5(3): 58–72

Seredin, V. V., Finkelman, R. B., 2008. Metalliferous Coals: A Review of the Main Genetic and Geochemical Types. *International Journal of Coal Geology*, 76(4): 253–289. https://doi.org/10.1016/j.coal.2008.07.016

Shawe, D. R., 2011. Uranium-Vanadium Deposits of the Slick Rock District. U.S. Geological Survey Professional Paper 576-F, Colorado

Shmariovich, Y. M., Natal'Chenko, B. I., Brovin, K. G., 1988. Conditions of Formation of Multi-Element Stratabound Infiltrational Mineral Deposits. *International Geology Review*, 30(6): 668 – 675. https://doi.org/10.1080/00206818809466047

Sibson, R. H., Moore, J. M. M., Rankin, A. H., 1975. Seismic Pumping—A Hydrothermal Fluid Transport Mechanism. *Journal of the Geological Society*, 131(6): 653–659. https://doi.org/10.1144/gsjgs.131.6.0653

Skirrow, R. G., Mercadier, J., Armstrong, R., et al., 2016. The Ranger Uranium Deposit, Northern Australia: Timing Constraints, Regional and Ore-Related Alteration, and Genetic Implications for Unconformity-Related Mineralisation. *Ore Geology Reviews*, 76: 463–503. https://doi.org/10.1016/j.oregeorev.2015.09.001

Sozinov, N. A., 1966. Uranium-Germanium Ore in Miocene Coal-Bearing Strata. Materialy Koordinatsionnogo Soveta, Vol. 2. VIMS, Moscow. 55–59 (in Russian)

Thomas, P. K., Thomas, T., Thomas, J., et al., 2014. Role of Hydrothermal Activity in Uranium Mineralisation in Palnad Sub-Basin, Cuddapah Basin, India. *Journal of Asian Earth Sciences*, 91: 280–288. https://doi.org/10.1016/j.jseaes.2014.02.013

Turner-Peterson, C. E., Fishman, N. S., 1986. Geologic Synthesis and Genetic Models for Uranium Mineralization in the Morrison Formation, Grants Uranium Region, New Mexico. A Basin Analysis Case Study. *American Association of Petroleum Geologists*, 1986: 357–388. https://doi.org/10.1306/st22455c21

Valsardieu, C., 1971. Cadre Géologique et Paléogéographique des Minéralisations de Charbon, de Cuivre et d'uranium de la Région d' Agadès (République du Niger): [Dissertation], Nice University, Nice. 518

Velichkin, V. I., Kushnerenko, V. K., Tarasov, N. N., et al., 2005. Geology and Formation Conditions of the Karku Unconformity-Type Deposit in the Northern Ladoga Region (Russia). *Geology of Ore Deposits*, 47(2): 87–112

Verma, M. B., Maithani, P. B., Chaki, A., et al., 2009. Srisailam Sub-Basin, a Uranium Province of Unconformity-Related Deposits in Andhra Pradesh Case Study of Chitrial Uranium Exploration, Nalgonda District, *Current Science*, 96(4): 588–591

Weber, F., 1968. Une Série Précambrienne du Gabon: le Francevillien. Sédimentologie, Géochimie, Relations avec les Gîtes Minéraux Associés. *Mémoire Service Carte Géologique de l' Alsace Lorraine*, 28: 238

Weissmann, G. S., Hartley, A. J., Scuderi, L. A., et al., 2013. Prograding Distributive Fluvial Systems—Geomorphic Models and Ancient Examples. New Frontiers in Paleopedology and Terrestrial Paleoclimatology: Paleosols and Soil Surface Analog Systems. *Society for Sedimentary Geology*, 104: 131–147. https://doi.org/10.2110/sepmsp.104.16

Wenrich, K. J., Lach, P., Cuney, M., 2018. Rare-Earth Elements in Uraninite-Breccia Pipe Uranium District, Northern Arizona, USA. International Symposium on Uranium Raw Material for the Nuclear Fuel Cycle: Exploration, Mining, Production, Supply and Demand, Economics and Environmental Issues (URAM-2018), IAEA, Vienna

Wenrich, K. J., Titley, S. R., 2008. Uranium Exploration for Northern Arizona (USA) Breccia Pipes in the 21st Century and Consideration of Genetic Models. In: Spencer, J. E., Titley, S. R., eds., Ores and Orogenesis: Circum-Pacific Tectonics, Geologic Evolution, and Ore Deposits. *Arizona Geological Society Digest*, 22: 295e309

Wülser, P. A., Brugger, J., Foden, J., et al., 2011. The Sandstone-Hosted Beverley Uranium Deposit, Lake Frome Basin, South Australia: Mineralogy, Geochemistry, and a Time-Constrained Model for Its Genesis. *Economic Geology*, 106(5): 835–867. https://doi.org/10.2113/econgeo.106.5.835

Yang, D. G., Wu, J. H., Nie, F. J., et al., 2020. Petrogenetic Constraints of Early Cenozoic Mafic Rocks in the Southwest Songliao Basin, NE China: Implications for the Genesis of Sandstone-Hosted Qianjiadian Uranium Deposits. *Minerals*, 10(11): 1014. https://doi. org/10.3390/min10111014

Young, R. G., 1964. Distribution of Uranium Deposits in the White Canyon-Monument Valley District, Utah-Arizona. *Economic Geology*, 59(5): 850–873. https://doi.org/10.2113/gsecongeo.59.5.850

Zhang, C. Y., Nie, F. J., Jiao, Y. Q., et al., 2019. Characterization of Ore-Forming Fluids in the Tamusu Sandstone-Type Uranium Deposit, Bayingobi Basin, China: Constraints from Trace Elements, Fluid Inclusions and C-O-S Isotopes. *Ore Geology Reviews*, 111: 102999. https://doi.org/10.1016/j.oregeorev.2019.102999

Zhang, L., Liu, C. Y., Fayek, M., et al., 2017. Hydrothermal Mineralization in the Sandstone-Hosted Hangjinqi Uranium Deposit, North Ordos Basin, China. *Ore Geology Reviews*, 80: 103 – 115. https://doi. org/10.1016/j.oregeorev.2016.06.012

Zhang, L., Liu, C. Y., Lei, K. Y., 2019. Green Altered Sandstone Related to Hydrocarbon Migration from the Uranium Deposits in the Northern Ordos Basin, China. *Ore Geology Reviews*, 109: 482–493. https://doi.org/10.1016/j.oregeorev.2019.05.008

Zhao, L., Cai, C. F., Jin, R. S., et al., 2018. Mineralogical and Geochemical Evidence for Biogenic and Petroleum-Related Uranium Mineralization in the Qianjiadian Deposit, NE China. *Ore Geology Reviews*, 101: 273–292. https://doi.org/10.1016/j.oregeorev.2018.07.025

Zielinski, R. A., 1983. Tuffaceous Sediments as Source Rocks for Uranium: A Case Study of the White River Formation, Wyoming. *Journal of Geochemical Exploration*, 18(3): 285 – 306. https://doi. org/10.1016/0375-6742(83)90074-2